ELSEVIER

Coordination Chemistry Reviews
178–180 (1998) 529–564

COORDINATION CHEMISTRY REVIEWS

Aspects of anionic framework formation Clustering of p-block elements

Claude Belin *, Monique Tillard-Charbonnel

Laboratoire des Agrégats Moléculaires et Matériaux Inorganiques, CC015, Université Montpellier II, Sciences et Techniques du Languedoc, 2 Place Eugène Bataillon, 34095 Montpellier, cedex 5, France

Received 3 November 1997; accepted 16 June 1998

Contents

Abstract

High electron delocalization and coordination numbers are typical of metals. For alloys in which the electronegativities of the components are sufficiently different, electron transfer brings the electronegative elements into new electronic configurations. This transforms metallic architectures either into classical anionic frameworks (Zintl phases) obeying the octet and

* Corresponding author. Fax: +33 4 67143304; e-mail: cbelin@univ-montp2.fr

PII S0010-8545(98)00168-4

$8-N$ valence rules, or into various complex networks in which classical valence rules no longer hold. Intermediate phases with partially delocalized bonding may form with clusters which mostly satisfy Wade's electron-counting rules. Generally, these phases have closed-shell electronic structures and the expected semiconducting properties. However, some of them display poor metallic behaviour owing to a few additional and somewhat delocalized electrons.

The intermetallic chemistry of group 13 elements with alkali metals provides an interesting overview of various structural and electronic situations. Bonding within naked clusters and anionic cages of p-block elements clearly illustrates the transition between the metallic and molecular states.

Keywords: Anionic frameworks; Clusters; Electronic structures; Intermetallic compounds; Zintl anions; Zintl phases

1. Background

The recent discovery of quasi-crystals, intermetallic compounds with very unusual structural and physical properties, represents an extraordinary event and an encouraging sign that metallurgy and intermetallic chemistry are not out-of-date sciences. Since the macroscopic properties of metals and alloys were of early interest to man, their hidden structures and physical properties have for a long time remained veiled. The information acquired in this century due to progress in various analytical techniques, in particular the discovery of X-ray diffraction, the application of atomic theories and the development of quantum mechanical calculation programs running on huge computers, has boosted research into fields expected to have a bright future in technology. We cite enormous amounts of research relative to superconducting materials, expected to revolutionize our way of life in the next millenium. About 80 elements of the periodic classification are metallic, and a great number of them may be alloyed. For binary alloys, the theoretical number of 3000 combinations is considerable, but this number reaches 80 000 and 1 500 000 for ternary and quaternary alloys, respectively. In the near future, struggling in the jungle of metal combinations will be less necessary, as it is likely that sophisticated simulation programs associated with huge electronic databases will indicate direct routes towards alloys and intermetallic phases with the desired properties. The cost of research will, concomitantly, be considerably reduced, but at the expense of the imagination of the chemist.

1.1. Intermetallic compounds

Intermetallic compounds form between elements which are somewhat different in size, electronegativity and crystal structure. Their formation has been analysed through valuable pioneering research. In a statistical review of intermetallic compounds, Laves formulated three basic principles: closest packing, greatest symmetry, and maximum number of connections between atoms [1]. Nowadays, the term "Laves phase" is used for certain alloys having the composition AB_2, where A is greater than B. A typical example is $MgCu_2$ which adopts a cubic structure (C15

type), and variants are hexagonal $MgZn_2$ (C14 type) and $MgNi_2$ (C36 type), which is a mixture of C15 and C14 slabs alternating along a hexagonal axis, and which may therefore be considered as a polytype. Laves phases belong to the tetrahedrally close-packed (tcp) structure types. Hume-Rothery [2] used the average valence electron per atom ($\bar{Z}$) to classify numerous phases having structures of different types of brass (CuZn alloys). In these phases, the d bands are entirely filled and the s and p electrons partially fill bands near the Fermi surface. $\bar{Z}$ is calculated by dividing the number of valence (s, p) electrons by the number of atoms in the formula. The disordered fcc α-phase ($Cu_{1-x}Zn_x$, $0<x<0.38$) is observed for $\bar{Z}$ up to 1.38, the bcc β-phase (CuZn, Cu_3Al, Cu_5Sn, etc.) exists around 1.48 ($\sim$21/14), the cubic γ-phase (Cu_5Zn_8, Cu_9Al_4, etc.) around 1.62 ($\sim$21/13) and the hcp ϵ-phase ($CuZn_3$, Au_5Al_3, etc.) around 1.75 (21/12). Some of these phases may indeed have a certain range of stoichiometry while retaining the same structure.

More recently, Pearson [3,4] has described intermetallic phases in terms of frameworks. The cfc structure of the $MgCu_2$ Laves phase [5] can then be seen as formed from two types of CN12 and CN16 Frank–Kasper polyhedra, i.e. Mg_6Cu_6 icosahedra around Cu atoms and Mg_4Cu_{12} icosioctahedra around Mg atoms (see Fig. 1).

Using bond orders, Pearson calculated the electron concentrations around each type of atom and classified intermetallic phases into five groups:

(1) Compounds with dense packing where the number of electrons required to satisfy bond formation between close neighbours frequently exceeds the number of valence electrons provided by component atoms (includes Laves phases).
(2) Compounds in which the band structure energy is a large fraction of the total energy. Structural changes are observed for particular values of electron concentration per atom (includes Hume-Rothery phases).
(3) Valence compound compositions where normal chemical valence rules are satisfied (e.g. Sb_2Se_3).
(4) Framework structures in which all atoms form a common framework. The distances to nearest neighbours agree with the Pauling formula for bond orders. In these compounds, valence rules are not obeyed, nor are specific electron concentrations satisfied.

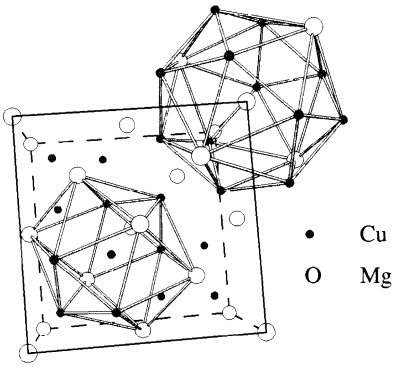

Fig. 1. $MgCu_2$ structure type (*Fd*3*m*). Coordination shells around atoms are indicated.

(5) Hybrid framework structures (for example $BaAl_4$) in which some atoms form partial frameworks having a definite relationship to the number of valence electrons.

Pauling's approach to chemical bonding within intermetallic compounds is based on some covalence considerations and was further developed in his resonating valence bond theory of metals and alloys [6,7].

As in molecules, polar bonding in intermetallic compounds should be observed when the component atoms have very different electronegativities. This is the case for compounds containing electropositive elements (alkali or alkaline–earth metals) and moderately electronegative p-block elements. Chemical bonding within these compounds is intermediate between ionic, metallic and covalent. The term "Zintl phase" was used for the first time by Laves in recognition of the pioneering work of Zintl [8–12]. NaTl has often been referred to as a typical Zintl phase. Its structure is formed from two interpenetrating diamond lattices (Na and Tl). Each Tl atom is tetrahedrally coordinated to other Tl, with the Tl–Tl bond significantly shorter (3.24 Å) than that in metallic hc α-Tl (3.42 Å, CN12) or bcc β-Tl (3.36 Å, CN8). Zintl considered NaTl as Na^+Tl^-, with Tl^- present not as a simple monoanion but as an extended 3D anionic framework, like the four-valence electron elements C or Si. According to this principle, in NaSi (Na^+Si^-) silicon forms a discrete tetrahedral aggregate Si_4^{4-} [13], isosteric with the P_4 and As_4 molecules in white phosphorus and yellow arsenic. In $CaSi_2$ [14,15], silicon (Si^-) forms puckered hexagonal layers as found in black phosphorus and grey arsenic. Exceptions exist: a framework of the NaTl type forms in $SrAl_2$ [16] but not in $SrGa_2$ [17]. In the latter, although having the same electron concentration, Ga atoms are not tetrahedrally bonded but form graphite-like layers. In these few examples, p-block elements form anionic frameworks which provide an octet of electrons, and it is likely that atomic size effects determine which of the different arrangements is adopted.

Klemm and Busmann [18] generalized the original idea of Zintl to any system in which electron transfer brings the electronegative element into a new electronic configuration, allowing a partial anionic lattice to be built in which the octet and $8-N$ rules are most often satisfied. Beyond Zintl phases containing single atoms with filled valence shells and classical salt structures, the Zintl–Klemm–Busmann concept elegantly applies also to phases having oligomeric and polymeric homo- or heteroanionic networks. The number of intermetallic phases now compiled under the heading of "Zintl phases" is enormous, and various types of chemical bonding are represented. In addition to its original linkage with classical valence rules, the extended Zintl concept can apply to some chemical bonding peculiarities such as those found in partially electron-delocalized cluster frameworks. Although the use of oxidation states or formal charges on individual atoms has proved invaluable in interpreting some partial anionic lattices, this approach is inapplicable to phases containing complex anionic frameworks or to phases with highly polarizing countercations. This is illustrated in the Li–Ga system in which six intermetallic compounds are known crystallographically: Li_2Ga, Li_3Ga_2, Li_5Ga_4, LiGa, Li_5Ga_9 and Li_2Ga_7 (Fig. 2). Only for LiGa, which is isostructural with NaTl, is the ionic formulation (Li^+Ga^-) consistent with the observed four-coordination for gallium.

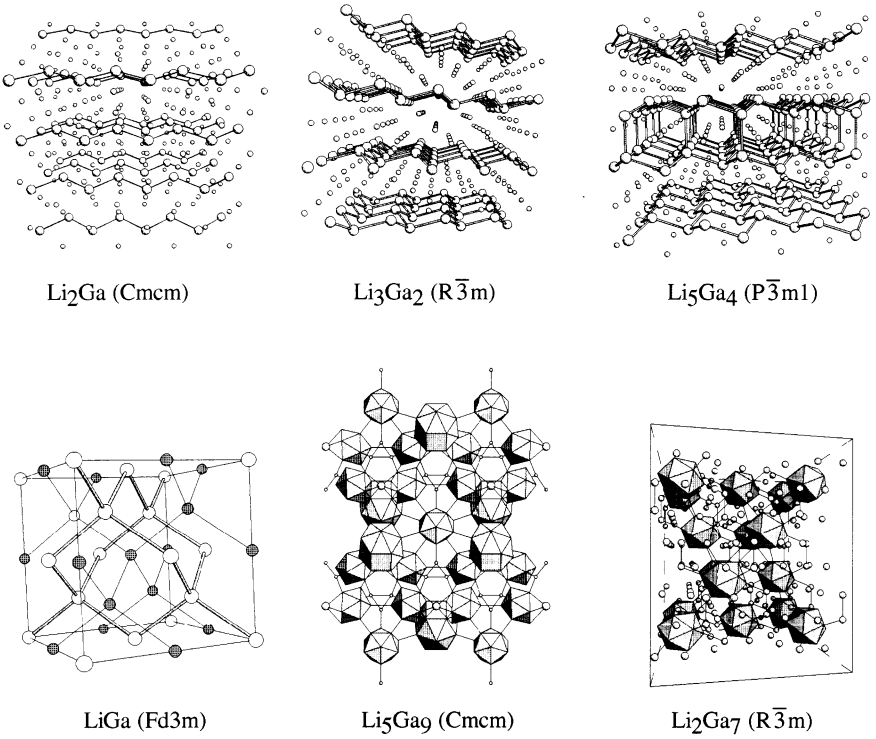

Fig. 2. Crystal structures of intermetallic phases in the Li–Ga system.

Li_3Ga_2 [19] displays puckered hexagonal layers of three-coordinated Ga atoms, the ionic charge per gallium atom would then be expected to be -2 instead of -1.5 to fulfil the octet rule. Two-bonded Ga atoms forms zig–zag chains in Li_2Ga [19], as does antimony in $CaSb_2$ [20,21], and the expected charge on gallium (-3) would exceed the calculated one (-2). Li_5Ga_4 [22] forms with twinned puckered hexagonal layers containing equal numbers of four-coordinated and three-coordinated gallium atoms. Although the compound is cleverly formulated as $2LiGa + Li_3Ga_2$, the -1.25 average charge on gallium is still less than that required (-1.5). In these Li-rich compounds, it is clear that some covalence of the anionic framework with lithium obscures our understanding of chemical bonding. Such compounds deserve further theoretical studies.

In the Ga-rich phases, Li_5Ga_9 [23] and Li_2Ga_7 [24], the paucity of electrons (-0.56 and -0.29 charge on Ga, respectively) is such that gallium atoms aggregate into clusters in order to maximize the number of shared electrons. According to the Zintl–Klemm–Busmann principle, their anionic frameworks can be interpreted in terms of interconnected clusters which fulfil special electron requirements (this will be developed in the following sections). The ionic formulation for Li_2Ga_7, i.e. $4Li^+$, Ga_{12}^{2-}, $2Ga^-$, indicates the anionic lattice to be formed by gallium icosahedra and isolated atoms, but gives no information on how they are interconnected.

1.2. Clustering of elements

The term cluster has been widely used during the last 20 years, in science (astronomy, mathematics, physics, chemistry, biology, etc.) to designate aggregates of things of the same kind. In chemistry, the term cluster refers to an aggregate of at least three metal atoms forming three metal–metal bonds (metal triangle). Clusters can be neutral, cationic or anionic, and exist as discrete units in either liquid phases or the solid state, or as building units forming larger networks in the solid state. Typical geometric figures described by metal atoms in clusters are triangles, tetrahedra, pyramids, octahedra, cubes, etc. in order to generate high degrees of connectivity.

The range of elements in the periodic table which display the ability to cluster is very impressive, but rare-earth and later main group elements are poorly represented. Molecular clusters mainly pertain to d-block metal chemistry. Complexes such as $Os_5(CO)_{16}$ [25], $Ni_6(CO)_{12}^{2-}$ [26] or $[Au_{13}(PMe_2\phi)_{10}Cl_2]^{3+}$ [27] are formed by a metallic core stabilized by surrounding organic ligands (CO, C_5H_5, phosphines, etc.) which modify the electronic configuration of the metals. That may provide specific chemical activities of interest in fields of catalysis and biological processes [28–30].

The conception and development of synthetic routes to homoatomic transition element clusters has been pioneered by Chini [31] and Johnson and Lewis [32], while Stone [33] and Vahrenkamp [34] have largely contributed to the discovery of new heterometallic compounds. Aspects of the homo- and heterometallic carbonyl clusters of the iron, cobalt and nickel triads have been reviewed by Braunstein and coworkers [35]. The earlier transition metals are generally associated with ligands such as O, S, Cl, Br, I, and give rise to an important structural type, i.e. 3D networks formed from octahedral metal units linked by halide or chalcogen bridges [36,37]. Among this class, the Chevrel–Sergent compounds (molybdenum chalcogenides) [38] have attracted much attention because of their physical properties, especially superconductivity.

Although lithium cluster chemistry bears some resemblance to that of transition metals, heavier alkali metals form typical suboxide clusters which are no longer stabilized by outer ligands but by interstitial oxygen atoms as exemplified in Rb_9O_2 and $Cs_{11}O_3$ [39,40] (Fig. 3).

A complete review of all cluster families is not the purpose of this article: here we focus on some aspects of the cluster chemistry of main group elements.

Main group elements are able to form a wide range of neutral or charged clusters. These can be seen as intermediate stages between single atoms or monoatomic ions and atomic arrays in the solid state, and are exemplified by As_4, S_8, C_{60}, Hg_3^{2+},

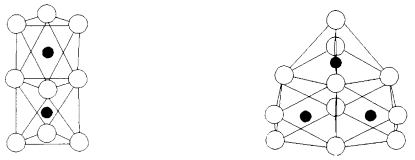

Fig. 3. Rb_9O_2 and $Cs_{11}O_3$ suboxide clusters.

Hg_4^{2+} [41], As^{3-} [42] and As_4^{2-} [43]. For Bi, S, Se and Te, both cationic and anionic clusters can be obtained, i.e. Bi_5^{3+} [44–46], Bi_8^{2+} [47], Bi_9^{5+} [48], S_8^{2+} [49], Se_4^{2+} [50], Te_6^{4+} [51,52], Bi_4^{2-} [53], Se_6^{2-} [54], and Te_3^{2-} [55], depending upon the synthesis routes (oxidation in Lewis acids, superacid solutions, reduction in basic solvents).

In recent years, many anions have been recognized in intermetallic phases of p-block elements with alkali or alkaline–earth metals. Some of them appear as discrete clusters, particularly for pnictogenides (As_6^{4-} in Rb_4As_6 [56], As_7^{3-} in Ba_3As_{14} [57], P_{11}^{3-} in Rb_3P_{11} [58]). As reported by von Schnering and Hönle [58], the number of polyanionic sublattices which exist in the phosphide family is very impressive, ranging from discrete polycyclic anions (P_7^{3-}) to 1D ($^1_\infty[P^-]$ helical chains), 2D ($^2_\infty[P_{10}^{2-}]$ linked tubes) and 3D ($^3_\infty[P_5^-]$ condensed P_6 and P_{10} cycles), polymeric anions.

In so far as the discovery of Tl_4^{8-} in Na_2Tl [59] dates back almost three decades, it seems puzzling today that the richness of alkali metal–thallium systems in discrete anionic clusters such as Tl_3^{7-}, Tl_4^{8-}, Tl_5^{7-}, Tl_6^{6-}, Tl_9^{9-}, Tl_{11}^{7-}, Tl_{13}^{10-}, Tl_{13}^{11-} [60–62] was unveiled so much later. This might reflect some disinterest of chemists owing to the high toxicity of this element.

2. Naked Zintl anions

In 1891, Johannis observed that some post-transition elements could be reduced in liquid ammonia by alkali metals [63,64]: the characteristic blue solution of sodium turned intense green in the presence of excess lead. $NaPb_4$ or $NaPb_2$ solid compounds were precipitated from this solution. Kraus [65] noted interesting electrolytic reactions for a green sodium–lead solution in liquid ammonia which produced lead plating on the anode. He proposed that the electrolyte contained Na^+ and Pb_2^- ions. A few years later, the green plumbide solution was controversially attributed by Smyth [66] to a mixture of Pb_2^- and Pb_3^- anions. Subsequently, Pb_9^{4-} was claimed by Kraus [67,68] to give the sodium–lead ammonia solution its green coloration. In 1931, Zintl [8–12] published impressive results on potentiometric titrations of sodium solutions in liquid ammonia by salts of post-transition elements (Sn, Pb, As, Sb, Bi, S, Se, Te) which led to the identification of numerous homoatomic polyanions.

In case of lead, the potentiometric and conductimetric titrations referred to the reaction

$$(4+2x)Na + xPbI_2 \rightarrow Na_4Pb_x + 2xNaI$$

Observation of two equivalent points in the titration curves provided evidence for the hepta- and nonaplumbide anions, Pb_7^{4-} and Pb_9^{4-}. Evaporation of ammonia from solutions of alkali metal–post-transition element alloys generally gave either amorphous products or phases already known in the corresponding alloy system. In 1970, Kummer and Diehl reported for the first time [69] isolation of a solid compound, i.e. $Na_4(en)_7Sn_9$ (en = ethylenediamine). It was characterized by ^{119}Sn

Mössbauer spectroscopy and the structure incompletely resolved by X-ray diffraction. Subsequently, other en-stabilized Zintl compounds $Na_4(en)_5Ge_9$ and $Na_3(en)_7Sb_7$ [70,71] have been obtained.

More recently, a general route to the stabilization of homopolyatomic anions has been proposed by Corbett and Edwards [72]. They used the 2,2,2-crypt [73] as a sequestering agent of alkali metal countercations, so preventing electron transfer from the anionic moieties back to the polarizing cations and further reversion to the classical alloy phase {crypt(2,2,2)=4,7,13,16,21,24-hexaoxa-1,10-diazobicyclo[8,8,8]hexacosane, $N(C_2H_4OC_2H_4OC_2H_4)_3N$}.

This synthetic route has allowed isolation of numerous homopolyatomic anions, such as Ge_5^{2-} [74], Ge_9^{2-} [75], Ge_9^{4-} [75], Ge_9^{3-} [76,77], Ge_{10}^{2-} [78], Pb_5^{2-} [79], Pb_9^{3-} [77,80], Pb_9^{4-} [80], Sn_5^{2-} [79], Sn_9^{3-} [81], Sn_9^{4-} [81], Sb_4^{2-} [82], Sb_7^{3-} [82,83], Sb_{11}^{3-} [84], Bi_4^{2-} [53], As_7^{3-} [85], As_{11}^{3-} [86], As_{22}^{4-} [87] and Te_3^{2-} [55], and heteroatomic anions such as $Pb_2Sb_2^{2-}$ [88], $Tl_2Te_2^{2-}$ [89], $TlSn_8^{3-}$ [90], $TlSn_9^{3-}$ [90], $As_2Se_6^{2-}$ [91], $As_2Te_6^{2-}$ [92], $As_{11}Te^{3-}$ [93], $Pb_2Te_3^{2-}$ [94], $Pb_2Se_3^{2-}$ [95], $Sb_2Se_4^{2-}$ [96], $As_2S_4^{2-}$ [96], $As_{10}Se_3^{2-}$ [97], $As_4Se_6^{2-}$ [96], $Sn_4Se_{10}^{4-}$ [98], the structures of which have been accurately determined (Figs. 4 and 5).

2.1. Summary of synthetic routes to Zintl anions

2.1.1. Extraction from Zintl phases and complexation of alkali metal cations by sequestering agents (crown ethers, bicyclic cryptands) in basic polar solvents

The use of binary A_xM_y or ternary phases $A_xM_yM'_z$ (A=alkali metal and M, M′=post-transition element) may afford isolation of homo- or heteroatomic anions. For example, the compound $[(2,2,2\text{-crypt},Na^+)_2, As_2Se_6^{2-}]$ was obtained by dissolu-

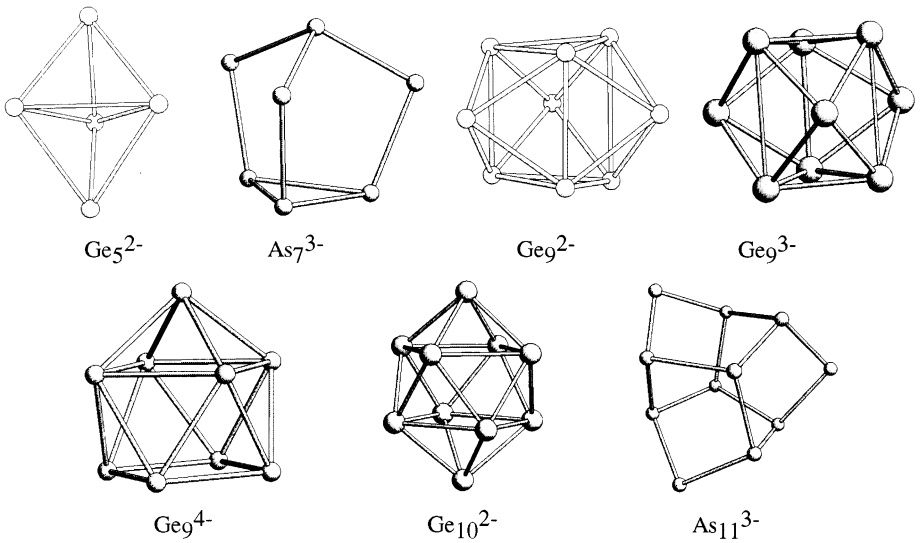

Fig. 4. Homoatomic anions of arsenic and germanium.

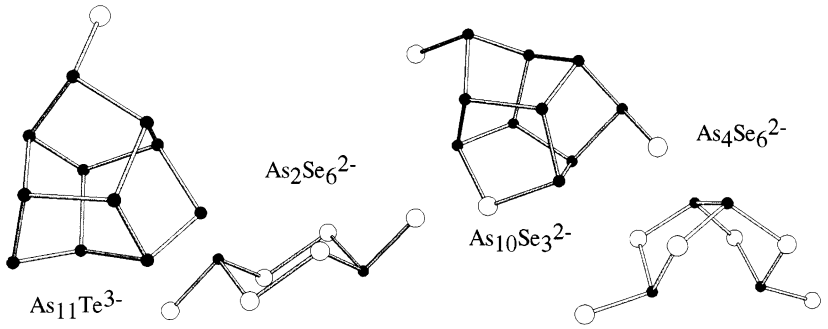

Fig. 5. Some heteroatomic anions in the arsenic chalcogenide family.

tion of $NaAs_2Se_3$ in en and complexation by 2,2,2-crypt [91]. $As_2Se_6^{2-}$, which can be obtained from several types of synthesis, has proved to be a very stable anion: for example, dissolution of As_4Se_4 in en/DMF cleaves an As–As bond and forms the $As_4Se_6^{2-}$ anion, and the addition of K_2Se_3 breaks the remaining As–As bond and produces $As_2Se_6^{2-}$ [99].

Alternatively, a binary alloy solution can be oxidized by an electronegative element (Se, Te), smooth oxidation of a KAs_2 solution in en by Te leads to the $As_{11}Te^{3-}$ anion [93].

2.1.2. Reaction of post-transition elements, of their salts and oxides with reducing agents (alkali metals, KC_8, etc.) in basic polar solvents

In a typical experiment, a solution of As_4Se_4 in en reacted with K to give an orange–red solution and a precipitate of K_2Se. Filtration, then addition of tetraphenylphosphonium bromide (countercation exchange) led to an intense red solution and a precipitate of KBr. A part of the filtered solution was immediately evaporated and gave red crystals of $(P\phi_4)As_7Se_4$ [100], while red crystals of $(P\phi_4)_2As_{10}Se_3$ [101] were obtained from another part of the solution after standing for several days.

2.1.3. Electrochemical production of Zintl anions

Haushalter and coworkers [102,103] recently showed that Zintl anions could be electrochemically produced without reducing chemicals or alkalides. $Sb_4Te_4^{4-}$ and $Sb_9Te_6^{3-}$ were obtained by cathodic dissolution of the Sb_2Te_3 compound. The syntheses are accomplished in en solutions of tetraalkylammonium salts, these electrolytes providing countercations. During electrolysis, the nickel anode is consumed into $NiBr_2$ while two compounds crystallize successively in the cathodic chamber. The $Sb_4Se_6^{2-}$ anion has been obtained by this electrochemical method [104], but also by a more classical chemical route [105]. $Sn_4Se_{10}^{4-}$ [106] is another example of an anion which can be obtained by electrochemical synthesis.

2.2. Electron counting and chemical bonding within clusters

Preliminary understanding of chemical bonding within clusters was promoted in the early 1950s by the conjunction of X-ray crystal structure determinations and semi-empirical molecular orbital calculations. Using LCAO methods, Longuet-Higgins and Roberts [107,108] have given an interpretation of the chemical bonding within metallic borides MB_6 (3D network of interconnected boron octahedra) which could not be described in terms of purely metallic or purely covalent bonding. They also investigated the stability of a regular boron icosahedron and were able to predict the structure of the $B_{12}H_{12}^{2-}$ boron hydride [107,108]. Boranes and carboranes are considered as electron-deficient clusters in the sense that they have insufficient electrons to form localized 2c–2e bonds along polyhedra edges. In a delocalized approach for $B_{12}H_{12}^{2-}$, an sp hybrid orbital is assigned to each boron atom which points radially outside the cluster and is involved in bonding with a hydrogen ligand. Three atomic orbitals per boron atom remain for skeletal bonding, i.e. one sp hybrid orbital which points towards the centre of the cluster and two p orbitals, tangential with respect to the surface of the cluster. In a simplified description, the 12 inward sp hybrid orbitals combine into one bonding and 11 antibonding molecular orbitals. The 24 tangential p orbitals combine pairwise to give 12 bonding and 12 antibonding MOs. The $B_{12}H_{12}^{2-}$ icosahedral cluster is stabilized with 26 electrons (13 filled levels) and has a closed-shell electronic configuration.

In order to describe chemical bonding in boranes, Lipscomb has elaborated an ingenious topological treatment termed *styx* [109] which is based on multicentre localized bonding (2c–2e and 3c–2e bonds). Bonding in boranes can usefully be described in s B–B–B bonds, t B–H–B bonds, y B–B bonds and x extra B–H bonds in addition to the one B–H bond each boron atom normally forms. The localized *styx* formalism has proved very efficient for the rationalization and prediction of most of the borane structures, but somewhat limited in interpreting bonding within higher and very symmetrical boranes.

20 years later, the topological electron counting (TEC) theory was published by Teo and coworkers, which gives electron counts for polyhedral clusters [110–114]. This approach is based on Euler's theorem ($E=V+F-2$ where E, V and F are numbers of polyhedron edges, vertices and faces) and the effective atomic number EAN rule (atoms in polyhedra can achieve an inert gas configuration: 8 and 18 valence electrons for main-group and transition-metal atoms, respectively). The number of cluster valence molecular orbitals CVMO is $8V-F+2+X$ where X is an adjustment factor corresponding to the number of "missing" antibonding orbitals if each edge is considered as a 2c–2e bond.

The polyhedral skeletal electron pair theory (PSEPT) developed chiefly by Wade and Mingos has been widely recognized as a hugely significant step forward in electron counting procedures. The term was first introduced by Mingos and coworkers [115] but the basic rules were initially formulated by Wade [116,117], and later developed by Mingos and Wales [118,119], Williams [120] and Rudolph [121]. Now they are often referred to as Wade's rules. PSEPT is based on the fact that a closed deltahedral cluster skeleton with n vertices requires $(n+1)$ electron pairs to fill the

$(n+1)$ skeletal bonding MOs (see Longuet-Higgins' work on $B_{12}H_{12}^{2-}$), such a polyhedron is called a *closo* cluster. The geometry related *nido* cluster has $n-1$ vertices and $n+1$ filled skeletal bonding MOs, the related *arachno* cluster has $n-2$ vertices and $n+1$ filled skeletal bonding MOs, the related *hypho* cluster has $n-3$ vertices and $n+1$ filled skeletal bonding MOs.

These rules have been supplemented by capping and condensation principles [122] which provide rationalization of large panoplies of structures built from simple polyhedral units (*closo*, *nido* or *arachno*). The skeletal electron count for a condensed cluster is equal to the sum of skeletal counts for the parent clusters minus that characteristic of the shared unit (atom, edge or face). These rules, apparently successful in transition metal chemistry, do not apply very well to main group clusters, where the final electron count depends on the shape of the condensed cluster and also on relative sizes of shared atoms. Capping of a triangular face of a *closo* deltahedral cluster may be considered as the condensation by face-sharing of this deltahedron with a tetrahedron. Application of the condensation rules indicates the resulting skeletal electron count to be unchanged.

2.3. Electron-deficient clusters

Pb_5^{2-}, Sn_5^{2-} [79] and Ge_5^{2-} [74], isoelectronic analogues of Bi_5^{3+} [44–46], display the trigonal bipyramidal geometry (D_{3h}) with a polyhedral electron count (PEC) of 22, of which 12 are skeletal electrons ($n+1$ pairs) and 10 are non-bonding electrons. In Pb_5^{2-}, bond lengths between equatorial atoms are 8% longer than axial-to-equatorial atom distances. Removal of an apical or an equatorial atom gives a tetrahedral (PEC = 20) or a butterfly cluster (PEC = 20 or 22). According to Mingos' rules for boranes, *nido* species are produced by removing one atom, that of highest connectivity, and the *nido* species derived from the M_5 cluster would therefore be the butterfly cluster. In the tetrahedral Si_4^{4-} anion, each atom is three-bonded by 2c–2e bonds and has one non-bonding pair. For this reason Si_4^{4-} is electron-precise as is its molecular analogue P_4. We will definitively adopt the term cluster for electron-deficient M_n aggregates which have less than $5n$ valence electrons. The terminology "electron-precise cages" is preferred for main group species with $5n$ valence electrons and three-bonded atoms (Si_4^{4-}, P_4, organic molecules such as C_4R_4-tetrahedrane, C_6R_6-prismane, C_8R_8-cubane, cuneane, etc.). Species having more than $5n$ valence electrons with atoms having lower coordinations and more than one lone pair will be referred to as electron-precise rings or chains.

The nine-atom cluster family is very exciting since it provides many examples of naked clusters for the Ge, Sn, Pb triad. Isoelectronic analogues in these series can be compared and information about bonding derived. These series include 20, 21 and 22 skeletal electron clusters.

To date, Ge_9^{2-} is the unique homoatomic representative of the 20 electron family; nevertheless, it is isoelectronic with $B_9H_9^{2-}$ [123] and with the heteroatomic analogue $TlSn_8^{3-}$. Ge_9^{2-} has been found, in association with the Ge_9^{4-} 22 skeletal electron cluster, in the mixed valent compound $(2,2,2\text{-crypt},K^+)_6Ge_9^{2-}$, Ge_9^{4-}, 2.5en. The tricapped trigonal prismatic Ge_9^{2-} *closo* cluster is slightly distorted from D_{3h} towards

C_{2v} symmetry, as indicated by a nearly 11% elongation of one of the three heights of the trigonal prism. Of course, crystal lattice effects might be responsible for the slight deformation of the 20 skeletal electron Ge_9^{2-} from D_{3h} symmetry. However, a LDFT (local density functional theory) optimization of the hypothetical Pb_9^{2-} cluster starting from D_{3h} geometry led to the more stable C_{2v} configuration [80].

The 22 skeletal electron clusters Ge_9^{4-}, Sn_9^{4-}, Pb_9^{4-} are *nido* species with capped square antiprismatic geometries close to C_{4v}. In these anions, one prism height is now 30–35% longer than the other two. Some fluxionality has been invoked for these anions in liquid state as observed by NMR and, in agreement, molecular orbital calculations for capped square antiprismatic C_{4v} and tricapped trigonal prismatic D_{3h} configurations have shown the energy barrier for the *nido* $C_{4v} \leftrightarrow$ *closo* D_{3h} interconversion to be very weak and less than 0.1% of the total orbital energies of either symmetry [124]. These M_9^{4-} clusters (C_{4v}) are isoelectronic with Bi_9^{5+} (crystallographic C_{3h} symmetry) which, instead, does not significantly deviate from D_{3h} symmetry (Fig. 6).

Ge_9^{3-}, Sn_9^{3-}, Pb_9^{3-} are 21 skeletal electron clusters which have been shown to be paramagnetic by EPR and magnetic susceptibility measurements. The geometry of Sn_9^{3-} deviates very slightly from D_{3h} symmetry (less than 1% deviation in prism heights). Ge_9^{3-} is clearly C_{2v} as is indicated by one of the prism heights which is markedly shorter (2.82 Å) than the other two (3.20 and 3.27 Å). The geometry of Pb_9^{3-} is close to C_{2v} with a 6% deviation in prism heights. In contrast to Ge_9^{3-}, it is striking that Pb_9^{3-} has one prism height longer (3.60 Å) than the other two (3.40 and 3.41 Å). For D_{3h} or pseudo-D_{3h} M_9 clusters, Corbett has shown that the best configuration-to-electron count correlation is given by height-to-edge length (h/e) ratio of the trigonal prism [124]. Mean ratios of 1.03 and 1.17 have been determined respectively for the 20 ($\sim D_{3h}$) and 22 ($\sim C_{4v}$) skeletal electron subgroups (Table 1). Calculated ratios for 21 skeletal electron clusters are 1.17 for Ge_9^{3-}, closer in value to that characteristic of the C_{4v} configuration, and 1.08 for Sn_9^{3-} and Pb_9^{3-}, the geometries of which are closer to D_{3h}.

Calculations at the extended Hückel level have been carried out for experimental and idealized geometries of Ge_9^{n-} clusters (Fig. 7). Ge_9^{2-} (C_{2v} experimental configuration) has a HOMO–LUMO separation of only 0.6 eV, with the LUMO (b_1) mainly σ antibonding along the trigonal prism heights, and π bonding within prism

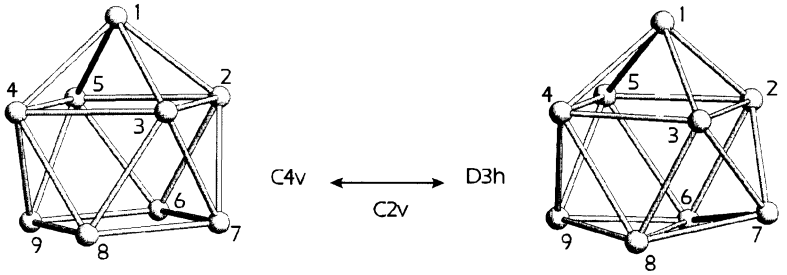

Fig. 6. Geometrical interconversion of M_9 cluster.

Table 1
Main geometric features of some M_9 clusters

Anion	Reference	~Symmetry	Skeletal electrons	Prism heights (Å)	*h/e*
Ge_9^{4-}	[75]	C_{4v}	22	2.70, 2.76, 3.64	1.18
Sn_9^{4-}	[81]	C_{4v}	22	3.23, 3.31, 4.21	1.17
Pb_9^{4-}	[80]	C_{4v}	22	3.35, 3.43, 4.33	1.16
Bi_9^{5+}	[48]	D_{3h}/C_{3h}	22	3.74, 3.74, 3.74	1.15
Ge_9^{3-}	[76]	C_{2v}	21	2.82, 3.20, 3.27	1.17
	[77]	C_{2v}	21	2.86, 3.15, 3.32	1.17
Sn_9^{3-}	[81]	D_{3h}	21	3.27, 3.31, 3.32	1.08
Pb_9^{3-}	[80]	C_{2v}	21	3.40, 3.41, 3.63	1.08
	[77]	C_{2v}	21	3.40, 3.41, 3.60	1.08
Ge_9^{2-}	[75]	C_{2v}	20	2.81, 2.86, 3.17	1.10
$TlSn_8^{3-}$	[90]	D_{3h}^{a}	20	3.15, 3.16, 3.30	1.03

[a] Ignoring thallium atom, *h/e* = height-to-edge length ratio.

bases and along cap-to-prism edges. In Ge_9^{3-}, the corresponding orbital is lowered in energy and becomes the single-occupied HOMO. The HOMO–LUMO separation is then 2.7 eV. The one-electron occupation of the HOMO increases the mean prism height and strengthens bonds within prism bases. Calculation for the capped square antiprismatic Ge_9^{4-} indicates a HOMO–LUMO separation of 3.1 eV. The HOMO is mainly bonding between the two squares of the antiprism. In the idealized C_{4v} geometry, these levels (HOMO and LUMO) are degenerate. Then, a C_{4v} geometry for Ge_9^{3-} (removal of one electron from the degenerate HOMO of Ge_9^{4-}) cannot be retained owing to Jahn–Teller distortion into C_{2v} geometry.

In Group 14, the uniqueness of the homoatomic Ge_{10}^{2-} [78] anion is surprising. It is noteworthy that the anion has been found to be disordered around the three-fold axis in a trigonal $P\bar{3}c1$ compound. Reassured by the observation that the crypt

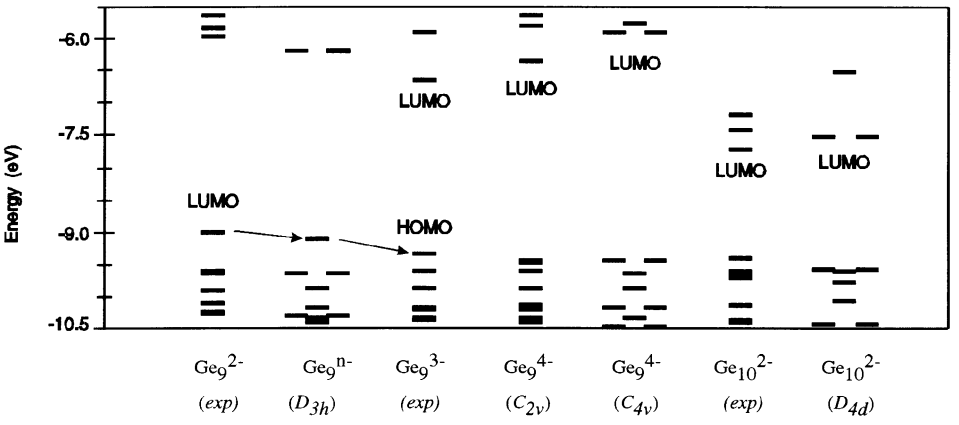

Fig. 7. Schematic MO energy diagrams for anionic germanium clusters in their experimental and idealized geometries.

cations could easily be resolved in the structure, positions of atoms within the anion were then deduced by deconvolution of the Fourier electron density. The bicapped square antiprismatic Ge_{10}^{2-} ($\sim D_{4d}$) is a *closo* 22 skeletal electron cluster isoelectronic with $B_{10}H_{10}^{2-}$ [125] and $TlSn_9^{3-}$ [90].

Tin and lead clusters have been shown to react with organometallic molecular fragments. The hitherto unknown *closo* Sn_6^{2-} could be stabilized as $Sn_6(Cr(CO)_5)_6^{2-}$ [126] by addition, *exo* at each vertex, of a $Cr(CO)_5$ two-electron acceptor ligand. In $M_9(Cr(CO)_3)^{4-}$ [127,128] with M = Sn, Pb, the nine-atom C_{4v} square antiprism is capped by the Cr atom of a $Cr(CO)_3$ electrophile ligand. In such a molecule, where a transition metal participates in skeletal bonding, the number of electrons n it supplies is $v+x-12$ (v = valence electrons of the transition metal, x = electrons provided by ligands). In this case, $n=0$ and Cr, which has three available orbitals, accepts six electrons from the open square face of the M_9^{4-} cluster (Fig. 8).

2.4. Electron-precise and electron-rich species: cages, rings and chains

Arsenic or combinations with chalcogen elements provide some beautiful examples of polycyclic anionic cages, such as As_7^{3-} [85], As_{11}^{3-} [86] (Fig. 4), $As_{11}Te^{3-}$ [93], $As_{10}Te_3^{2-}$ [87], $As_{10}Se_3^{2-}$ [101] and $As_{10}S_3^{2-}$ [96] (Fig. 5). In these anionic species the maximum coordination for arsenic is three, while chalcogen elements are two- or one-coordinated. Neutral arsenic chalcogenides such as As_4Se_4 [129], As_4S_5 [130], As_4S_3 [131] also exhibit geometries which allow their classification as cages.

Some anionic rings (mono- or bicyclic species) exist in the arsenic chalcogenide family, i.e. $As_2S_4^{2-}$ [96], $As_2Se_6^{2-}$ [91,99], $As_2Te_6^{2-}$ [92] and $As_4Se_6^{2-}$ [96]. Tin and antimony chalcogenides also form rings, as in $Sn_3Se_8^{4-}$ [132] and $Sb_4Se_6^{2-}$ [104] (not isostructural with $As_4Se_6^{2-}$). Very impressive also is the largest polycyclic anion $Sb_{12}Se_{20}^{4-}$ [133] (Fig. 9).

In similar fashion as for clusters, cages and rings can also react with organic ligands to form complexes such as $As_7(Cr(CO)_3)^{3-}$ [134], $P_7(FeCp(CO)_3)^{3-}$ [135], $Sn_2Se_4\phi_2^{2-}$ [136] (Fig. 8), P_7R_3 or $P_{11}R_3$ [$R=M^{IV}(Me_3)$] [58] or Sn_8R_8 (R = 2,6-diethylphenyl) [137] (Fig. 8).

Seemingly, the anion $As_7Se_4^-$ [97] is a cage with 15 bonds and 60 valence electrons, in which one arsenic atom is four-coordinated, raising the question as to whether or not it might be hypervalent (Fig. 10). Extended Hückel molecular orbital

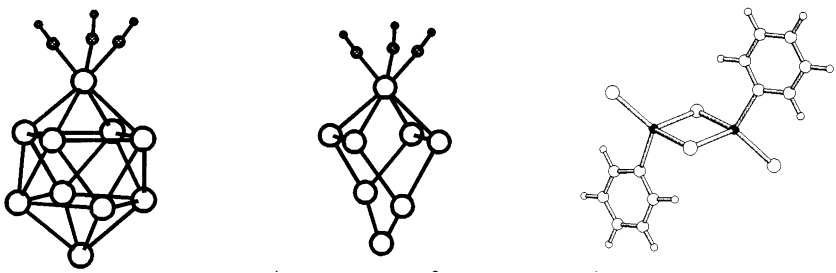

Fig. 8. $M_9(Cr(CO)_3)^{4-}$, $As_7(Cr(CO)_3)^{3-}$ and $Sn_2Se_4\phi_2^{2-}$ organometallic complexes formed from Zintl anions.

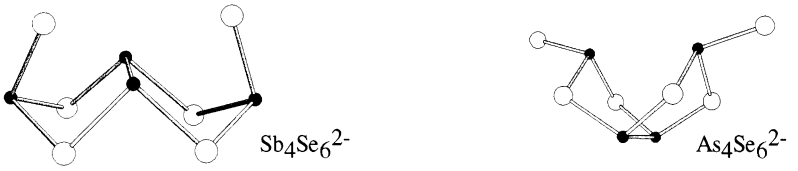

Fig. 9. Geometries of isoelectronic anions $Sb_4Se_6^{2-}$ and $As_4Se_6^{2-}$.

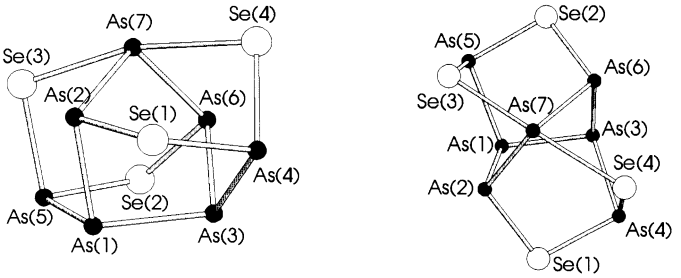

Fig. 10. Two views of the $As_7Se_4^-$ Zintl anion.

(EHMO) calculations have weakened the plausibility of hypervalence for the four-bonded As(7) atom, and we rather consider this anion as a hybrid between a cluster and a cage.

Overlap populations indicate single bonds between all atoms except As(7)–Se(3) and As(7)–Se(4) which have bond orders of 0.5. This gives a total of 28 bonding and 32 non-bonding electrons. Each arsenic atom, including the pseudo four-coordinated As(7), has a lone pair and selenium Se(1) and Se(2), two lone pairs. The remaining five non-bonding pairs are ascribed to the Se(3), Se(4) and As(7) atoms. Of the three sp^2 type orbitals at As(7) described in Fig. 11, one is a lone pair *exo* orbital, the other two are used in σ bonding (2c–2e) with As(2) and As(6) atoms. In a naïve localized molecular orbital scheme, bonding at the Se(3)–As(7)–Se(4) three-centre bond results from overlapping of the remaining p orbital of As(7), tangential to the anion surface with the Se(3) and Se(4) sp^3 type orbitals (Fig. 12). This gives one bonding (3c–2e), one non-bonding and one antibonding MOs.

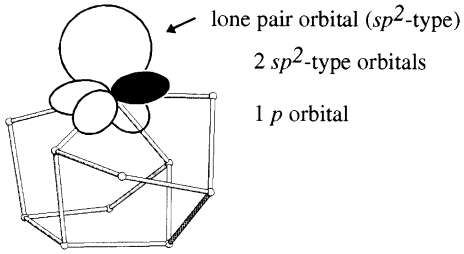

Fig. 11. Schematic representation of the As(7) atomic orbitals.

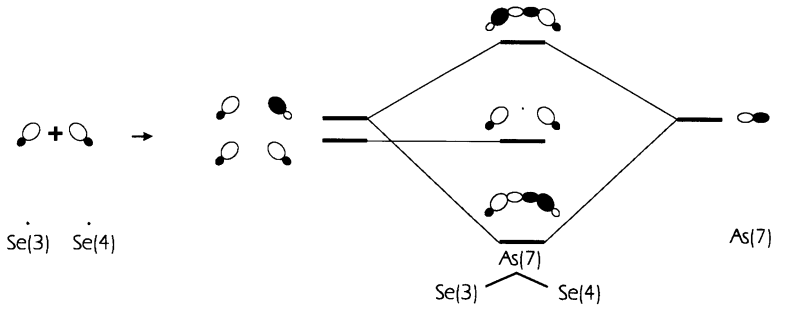

Fig. 12. Schematic orbital interactions within the Se(3)–As(7)–Se(4) edges.

Further reduction of $As_7Se_4^-$ anion by addition of two electrons would lead to the anion $As_7Se_4^{3-}$, the additional electrons would fill the antibonding level causing breaking of the 3c–2e bond and formation of a polycyclic anion with two As–Se exocyclic "handles" as in $As_4Se_6^{2-}$ [96] (see Fig. 9).

Bi_4^{2-} [53] and Sb_4^{2-} [82] have been isolated in crypt cation pnictogenide salts, and As_6^{4-} had earlier been discovered in Rb_4As_6 [56]. As_4^{2-} and As_6^{4-} have been characterized by EXAFS in solutions of K_3As_5 in en [43]. The 22 electron M_4^{2-} anion is square planar (D_{4h}) and, according to Wade's rules, it could be considered as an *arachno* species (derived from the octahedron) with seven SEPs (Fig. 13). However, a description of M_4^{2-} with seven bonding and four non-bonding molecular orbitals is unlikely. Rather, results from EHMO calculations show this electron-rich anion to be better described with six non-bonding and five bonding molecular orbitals (one π delocalized and four σ bonds). The D_{6h} planar hexagonal As_6^{4-} with 34 valence electrons does not satisfy Wade's requirements for an *arachno n*-atom species (polyhedral electron count $4n+6=30$) and must be described with one π delocalized and six σ bonds plus 10 non-bonding pairs (in agreement with Lewis notation).

Conversion of the tetrahedral 20 electron M_4 (As_4, Si_4^{4-} [13], Pb_4^{4-} [118,119] Tl_4^{8-} [59], $Sn_2Bi_2^{2-}$ [88], $Pb_2Sb_2^{2-}$ [88]) into the square 22 electron species (As_4^{2-} [43], Bi_4^{2-} [53], Te_4^{2+} [138–140], Sb_4^{2-} [82]) has been extensively analysed by MO calculations [141,142]. A two-electron reduction of the tetrahedral Si_4^{4-} breaks one edge of the tetrahedron leading to the 22 electron "backbone" butterfly Si_4^{6-} (C_{2v}) [143]. At the other end, folding of 30° about a diagonal of the square M_4 (D_{4h}) may lead to an open butterfly (C_{2v}) with 20 valence electrons as in $Tl_2Te_2^{2-}$ [89] (Fig. 13). Here, the heteroatomic nature of the anion and the difference in the

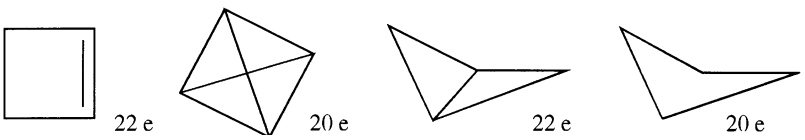

Fig. 13. Various geometrical configurations for M_4 species.

electronegativities of Tl and Te are responsible for this surprising two-electron decrease in the electron count.

A very large variety of electron-rich cycles and chains is observed in the chemistry of chalcogens (Se_8, Se_8^{2+} [144], Te_5^{2-} [54], Te_3^{2-} [55], Se_6^{2-} [54]), but no element shows as many different structures as sulphur. The crystal structures contain different S_n units ($n=6$, 7, 8, 10, 11, 12, 13, 18, 20, …, ∞). In the S_8 ring, in which bonding can be described with an electron-precise scheme, two electrons per S atom are involved in single bond formation with two adjacent sulphur atoms while the other four electrons are accommodated on two stereoactive lone pairs. Oxidation to S_8^{2+} increases connectivity through transannular interaction which occurs with a folding of the ring.

The chemistry of Te-rich telluride compounds has been particularly productive in recent years [144,145]. Many chain-like Te_n^{2-} can form, reminiscent of the infinite helices of the stable elemental form. The smallest one is Te_3^{2-}, but Te increases its coordination beyond two in most of the tellurium anions. The versatility of tellurium is well exemplified by the square planar structural unit (Te_5^{n-}) which can reorganize into infinite 1D to 3D anionic networks.

3. Clusters, building units in solid state chemistry

The remarkable richness and variety of clusters and cluster frameworks found in the intermetallic chemistry of alkali metals and Group 13 elements (particularly the Ga, In and Tl triad) has stimulated our interest in understanding various problems such as stoichiometry, structure, chemical bonding and interpreting the properties of these unusual compounds. Examination of intermetallic phases below will provide strong support to the basic Zintl principle of electron donation from alkali metals to electronegative elements.

Although a few examples of discrete clusters have been reported, gallium and indium display a general trend of forming extended anionic cluster frameworks, i.e. electron-deficient metal aggregates which are generally interconnected through classical 2c–2e bonds resulting in electron-poor (delocalized bonding) and electron-precise (localized bonding) structural domains. On the other hand, thallium chemistry is very rich in isolated cluster moieties reminiscent of boron chemistry. The following sections will mainly deal with gallium intermetallic phases. Since extensive work on indium and thallium intermetallic phases has recently been reviewed by Corbett [60], only a few examples of interest in these families will be discussed here.

The α-Ga structure has been described [146] as a molecular metal with covalently bonded Ga_2 molecular units. This trend to covalence is enhanced when gallium is reduced in intermetallic phases containing electropositive elements (alkali metals). Only a few additional electrons are needed to form, with gallium, aggregates which are typical of elemental boron.

3.1. Clustering in binary gallium phases

The electronic dependence is exemplified in the Li–Ga system (see Fig. 2). Gallium clusters form anionic lattices which adapt their structure to actual electron concentrations: gallium zig–zag chains in Li_2Ga, puckered layers in Li_3Ga_2 and Li_5Ga_4, and 3D networks in LiGa (diamond lattice), Li_5Ga_9 and Li_2Ga_7 (interconnected clusters).

The structure of MGa_7 (M = Rb, Cs) [147–149] contains icosahedra and four-bonded Ga atoms (Fig.14). Each icosahedron is connected to six other icosahedra by 3c–2e bonds forming flat slabs which are interconnected through Ga_2 "dumbbells" by 2c–2e bonds. The ionic formulation $2M^+$, Ga_{12}^0, $2Ga^-$ brings out some similarity to the neutral icosahedron layer of α-rhombohedral boron. Each icosahedron has 26 electrons for skeletal bonding and a total of 24 electrons in *exo* bonds. This gives a PEC of 50, as expected for a *closo* 12-atom cluster. Since electrons involved in *exo* bonding are shared by two (2c–2e bonds) or three (3c–2e bonds) adjacent units, the number of electrons each icosahedron contributes to the bonding (VEC) is 36 ($26+6\times2+6\times2/3$). Oxidation of the MGa_7 phase may be achieved by removing the reduced Ga atom, slabs would then be directly connected (2c–2e bonds). This restores the structure of α-rhombohedral boron.

Although the Li_2Ga_7 structure [24] looks different, it can be shown to derive from that of MGa_7 by local reduction. In the MGa_7 structure, there are two electron-deficient areas: icosahedra (26 skeletal electrons for 30 bonds, i.e. 0.86 electrons per edge) and 3c–2e bonds (0.66 electrons). Reduction (by incorporation of a supplementary alkali metal) would break the 3c–2e into 2c–2e bonds. Reorganization of the icosahedron slab (in MGa_7) into an antiprismatic arrangement while retaining the rhombohedral symmetry and four-bonded Ga_2 dumbbells leads to the structure of Li_2Ga_7 which can be formulated as $4Li^+$, Ga_{12}^{2-}, $2Ga^-$. Increase of the number of countercations requires tuning their size down to the smaller lithium ion. Further reduction of these anionic lattices is achieved on formation of smaller clusters which have, in comparison, higher electron concentrations. The tetragonal MGa_3 (M = K, Rb, Cs) phases [150–153] (ionic formulation $6M^+$, $2Ga_8^{2-}$, $2Ga^-$) contain 18 skeletal electron *closo* Ga_8 clusters (see Fig. 15). The tetragonal Rb_2In_3 structure [154] contains layers of 14 skeletal electron *closo* In_6 octahedra (Fig. 17 later).

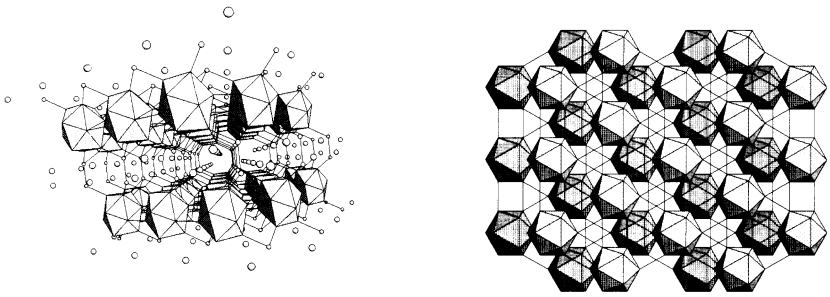

Fig. 14. The MGa_7 crystal structure ($R\bar{3}m$) viewed perpendicular (left) and along (right) the three-fold axis.

Reduction may also induce an increase of the number of isolated low-coordinated atoms. K_3Ga_{13} [155] is a good example of a structure formed by two kinds of *closo* clusters, icosahedra and octadecahedra (11 atoms), and both three- and four-bonded gallium atoms. It can be formulated as $6K^+$, Ga_{12}^{2-}, Ga_{11}^{2-}, $2Ga^-$, Ga^0. The 12-coordination of an icosahedron is achieved with two doubly-connected Ga_{12}, two Ga_{11} and six four-bonded gallium atoms (Fig. 15).

Also, 11-coordination for the octadecahedron is completed with two doubly-connected Ga_{11}, two Ga_{12}, three three-coordinated and two four-coordinated gallium atoms. With 2c–2e interpolyhedral bonds, K_3Ga_{13} has a closed-shell configuration [156]. Counts of 26 and 24 skeletal electrons for Ga_{12} and Ga_{11} fit Wade's electron requirements for *closo* polyhedra. Ga_{12} and Ga_{11} clusters are the isosteric inorganic core analogues of the boranes $B_{12}H_{12}^{2-}$ and $B_{11}H_{11}^{2-}$.

3.2. More electron-rich binary phases

As pointed out above for phases having a high alkali metal content (as in the Li–Ga system), strong reduction leads to lower dimensional arrangements for the electronegative element. There are some intermediate situations where frameworks containing electron-deficient clusters are still retained, but where the number of low-coordinated atoms has increased. These no longer occur as isolated atoms or "dumb-bell" units, but form polycyclic cages in which electron-precise bonding most often dominates. These cages have been termed spacers, as they space out the clusters. M_{15} is one of the most frequent spacers found in association with icosahedra in 3D networks related to the $MgCu_2$ structure type.

The two crystallographic forms of Na_7Ga_{13} [157,158] contain both icosahedra and Ga_{15} spacers. The difference between them arises from the different ways in which clusters are connected. In the rhombohedral (I) structure, one icosahedron has six non-*exo* bonded gallium atoms carrying a lone pair. Consequently, the VEC for this incompletely *exo* bonded icosahedron (type A) is 44 instead of 38 for the

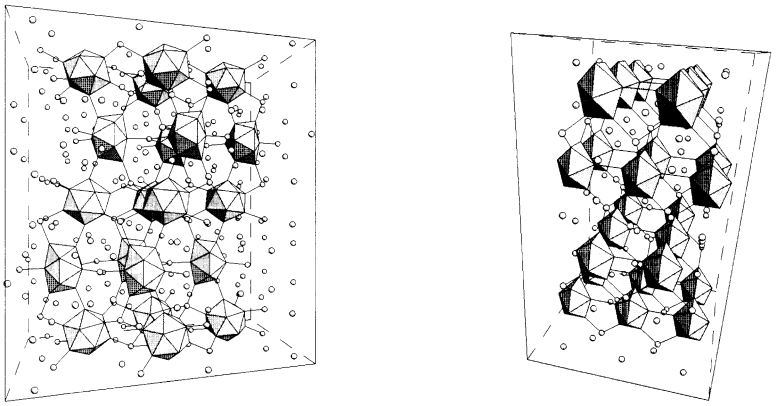

Fig. 15. Crystal structure of *Cmcm* K_3Ga_{13} (left) and $I\bar{4}m2$ KGa_3 (right).

12-*exo* bonded icosahedron (type B). All atoms of the Ga_{15} cages are *exo* bonded (Fig. 16).

In the Na_7Ga_{13}(II) [157,158] or $Na_{22}Ga_{39}$ [159] orthorhombic forms, icosahedron A, with only three non-*exo* bonded atoms, has a VEC of 41. Noteworthy are two atoms in the Ga_{15} cage, now non-*exo* bonded, which form a double bond (2c–4e). This is quite unusual in this kind of intermetallic phase. EHMO calculations [160] have shown that 46 skeletal electrons are required for stabilization of this 13-*exo* bonded Ga_{15} spacer (44 for the 15-*exo* bonded Ga_{15}). According to calculated overlap populations, this cage could schematically be described with $20 \times 2c–2e$, $1 \times 3c–2e$ and $1 \times 2c–4e$ bonds. Na_7Ga_{13} (I and II) are closed-shell compounds, while $Na_{22}Ga_{39}$, with one additional electron per formula unit, should be considered as an open-shell compound (Fig. 16).

In some phases having roughly the same electronic concentrations, spacers may coexist with *nido* icosahedra. In as much as *nido* clusters have higher electron concentrations per atom than their *closo* relatives, spacers lose the electron-precise character of bonding. In $Na_7In_{11.8}$ [161] and $Na_{15}In_{27.4}$ [162], anionic networks contain *nido* In_{11} and *closo* In_{16} clusters while in Li_5Ga_9 [23,163] *closo* Ga_{12} and

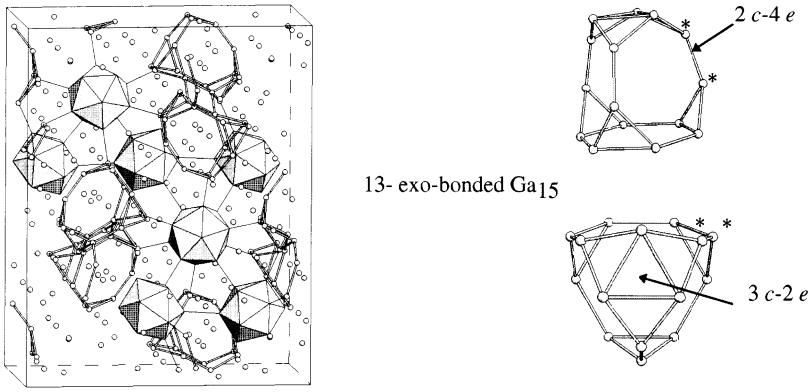

Fig. 16. The $Na_{22}Ga_{39}$ crystal structure (*Pnma*) and two views of the Ga_{15} spacer. * Refers to non-*exo* bonded atoms forming a double bond (2c–4e).

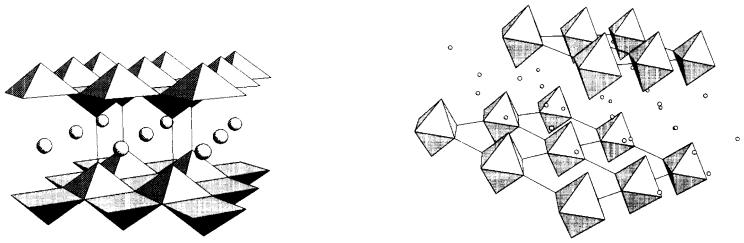

Fig. 17. Crystal structures of *I*4/*mmm* $NaGa_4$ and Rb_2In_3.

nido Ga_{11} clusters plus a Ga_{17} polyhedron are found (see Fig. 2), the latter being an intermediate between a cage and a cluster.

The binary intermetallic phases A_xM_y which have been reviewed are generally simple and mostly have anionic sublattices which contain clusters. However, $NaGa_4$ [157,158,164] does not really conform to this scheme. Its structure can be described as an infinite framework composed of edge-sharing square pyramids forming slabs interconnected by nearly 2c–2e bonds (see Fig. 17). Since the valence electron concentration per gallium atom in $NaGa_4$ (3.25) is very close to that in K_3Ga_{13} (3.23), which contains individual clusters, the reason why $NaGa_4$ crystallizes in the $BaAl_4$ structure type (the most common in intermetallic compounds) still remains obscure. This behaviour seems to be more dependent upon atomic sizes than valence electron concentrations [165,166].

3.3. Ternary and quaternary phases

In these intermetallic phases, introduction of alkali metals which are different in size leads to formation of complex anionic networks. In addition to clusters which now seem classical, more intricate polyhedra resulting from condensation of simple units are also found. Furthermore, in phases containing electron-poorer elements of Groups 11 and 12, electron concentrations are such that no low-coordinated atom is present. Instead, electron deficiency is overcome by condensation of clusters into fused (face-sharing) larger polyhedra.

In phases $Li_3Na_5Ga_{19.57}$ [167], $Li_9K_3Ga_{28.83}$ [168], $Na_{6.25}Rb_{0.6}Ga_{20.02}$ [169], anionic networks are formed (see Table 2) by twinned icosahedra, three- and four-bonded atoms, *closo* icosahedra and, as also found in Li_5Ga_9, $Na_7In_{11.8}$ or $Na_{15}In_{27.4}$, *nido* icosahedra. Here, the cluster of interest is the atom-deficient twinned icosahedron. It is compared to those found in AlB_{12} and α-tetragonal boron (see Fig. 18).

Table 2
Ternary and quaternary phases containing condensed icosahedra M_{21} and M_{28}

Compound	Valence electrons per heavy atom	Space group	Cluster type[a]	Isolated atoms	Atom-deficient
$Li_9K_3Ga_{28.83}$ [168]	3.42	*Cmcm*	M_{12}, M_{21}	none	yes
$Li_3Na_5Ga_{19.57}$ [167]	3.40	*Fmmm*	M_{12}, M_{21}	3b, 4b	yes
$Na_{6.25}Rb_{0.6}Ga_{20.02}$ [169]	3.33	*Fmmm*	M_{12}, M_{21}	4b	yes
$Na_{13}K_4Ga_{47.45}$ [170,171]	3.34	$R\bar{3}m$	M_{12}, M_{28}	none	yes
$Na_{14}K_{21}Cd_{17}Ga_{82}$ [172]	3.18	$R\bar{3}m$	M_{12}, M_{28}	none	yes
$Na_{17}Cu_6Ga_{46.5}$ [173]	3.10	$R\bar{3}m$	M_{12}, $M_{28}NM_{28}$	none	no
$Na_{17}Zn_{12}Ga_{40.5}$ [174]	3.10	$R\bar{3}m$	M_{12}, $M_{28}NM_{28}$	none	no
$Na_{34}Cu_7Cd_6Ga_{92}$ [175]	3.13	$R\bar{3}m$	M_{12}, $M_{28}NM_{28}$	none	no
$Na_{35}Cd_{24}Ga_{56}$ [176]	3.14	$Fd3m$	M_{12}, M_{16}	none	no
$Na_{36}Ag_7Ga_{73}$ [177]	3.27	$Fd3m$	M_{12}, M_{16}	none	no
$Li_{18}Cu_5In_4Ga_{31}$ [178]	3.32	$Fd3m$	M_{12}, M_{16}	none	no

[a] M, N = electronegative elements.

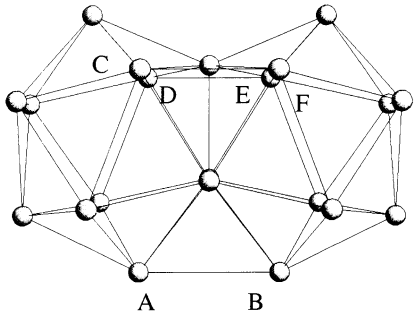

Compound	Ref.	Site occupations (%)					
		A	B	C	D	E	F
$Li_9K_3Ga_{28.83}$	[168]	51	0	16	16	100	100
$Li_3Na_5Ga_{19.57}$	[167]	60	60	53	53	53	53
$Na_{6.25}Rb_{0.6}Ga_{20.02}$	[169]	51	51	81	81	81	81
α- AlB_{12}	[180-182]	100	100	0	100	0	100
γ- AlB_{12}	[180-182]	100	100	0	0	100	100
α-tetragonal B	[180-182]	100	100	100	100	100	100

Fig. 18. Representation of the M_{21} twinned icosahedron. Atomic deficiencies for positions (A to F) are indicated for different compounds.

Condensation of two polyhedra by vertex-, edge- or face-sharing have been particularly well analysed by Mingos who established some rationalization principles [122] completing Wade's rules. The skeletal count for the twinned icosahedron would be $(2\times 26)-6=46$ electrons. This count has generally proven suitable with regard to the electron balances in these gallium intermetallic phases. The presence of defective atomic sites on clusters now raises the question as to whether or not the skeletal electron counts might be changed. These situations have been examined by Burdett and Canadell for the icosahedron [179]. If only one atom is missing, as a *nido* species it keeps the same skeletal electron count. However, when two adjacent atoms are removed (*iso-arachno* cluster), the skeletal count could be less than Wade's requirements for an *arachno* cluster. In the case of the above defective twinned icosahedra, no change in electron count has been observed.

Rhombohedral structures of $Na_{13}K_4Ga_{47.45}$ [170,171], $Na_{14}K_{21}Cd_{17}Ga_{82}$ [172] contain icosahedra and triply-fused icosahedra (or tri-icosahedra) (see Fig. 21). Interestingly, such a polyhedron exists in β-rhombohedral boron [180–182]. The triply-fused M_{28} polyhedron (Fig. 19) results from condensation by face-sharing of three icosahedra, each cluster shares one face with each neighbour. One atom (on the three-fold axis) is common to the three icosahedra. Owing to a general trend of atom deficiency, difficulties have been met with evaluating the skeletal electron count.

In $Na_{13}K_4Ga_{47.45}$, tri-icosahedra occur as inverted pairs through a $\bar{3}m$ centre and are connected by 2c–2e bonds to icosahedra. It has been crystallographically determined that only one of the six summits (ABC and inverted A′B′C′) is statistically occupied. Then, the inverted pair is considered as formed by a doubly-*nido* and a

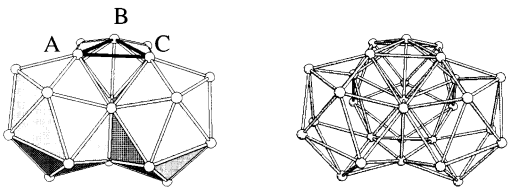

Fig. 19. Two representations of the M_{28} triply-fused icosahedron.

triply-*nido* tri-icosahedron (Fig. 20). These clusters, saturated with 18 hydrogen atoms to simulate *exo* bonding, have been analysed by EHMO calculations. Results show both polyhedra stabilized with 62 skeletal electrons. Yet the doubly-*nido* tri-icosahedron has a lone pair (HOMO) at the A apex.

In the case of a full Ga_{28} tri-icosahedron, the *exo* sp type AOs of atoms ABC would overlap into one bonding (a_1) and two antibonding (e) π type combinations (C_{3v} symmetry). The a_1 level lies at low energy and contributes into a 3c–2e bond. The antibonding combinations are pushed up in energy to the degenerate LUMO. The Ga_{28} skeletal count would be of 64 electrons (closed-shell configuration). 18 atoms are *exo* bonded and the number of valence electrons available for skeletal bonding is at least $(3\times 28)-18=66$ (zero oxidation state for Ga). Under these conditions, the two extra electrons would populate the degenerate antibonding level (LUMO). Such an electronic configuration would be energetically very unstable and prone to Jahn–Teller distortion. It would lead to elimination of two or three of the ABC atoms. Of course, the appropriate 64 electron count would be supplied by a Ga_{28}^{2+} cation, the existence of which is unlikely in such a highly reducing environment.

Energetic stabilization of two inverted units becomes possible when smaller and electron-poorer atoms, like Cu or Zn, are substituted for Ga. The geometry of the M_{28} tri-icosahedron is relaxed through enlarging the ABC triangle in such a manner that a heteroatom at the $\bar{3}m$ centre now coordinates the two inverted M_{28} units. EHMO and band calculations for phases $Na_{17}Cu_6Ga_{46.5}$ [173], $Na_{17}Zn_{12}Ga_{40.5}$

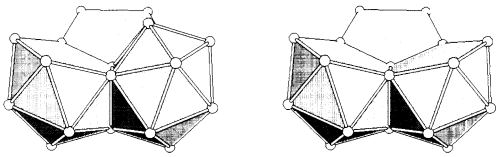

Fig. 20. The doubly-*nido* M_{26} and triply-*nido* M_{25} defective polyhedra.

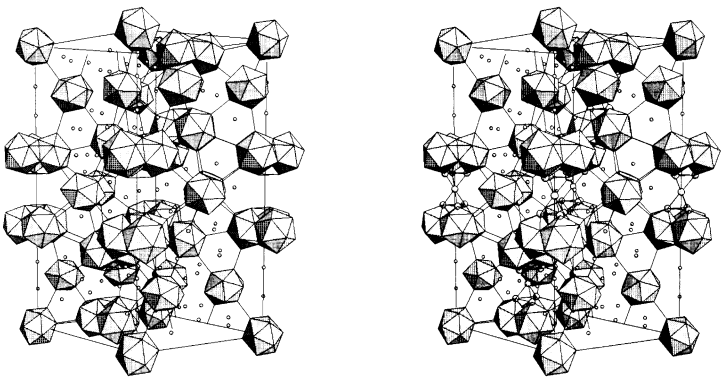

Fig. 21. Polyhedral packing in $R\bar{3}m$ $Na_{13}K_4Ga_{47.45}$ (left) and $Na_{17}Cu_6Ga_{46.5}$ (right) structures. They differ by the presence, in the latter, of a Cu atom between two M_{28} units.

[174], $Na_{34}Cu_7Cd_6Ga_{92}$ [175] indicate that the $M_{28}NM_{28}$ cluster requires 132 electrons for skeletal stabilization (see Fig. 21).

This stabilization can be readily described with a molecular orbital interaction diagram (Fig. 22). Six fragment orbitals, *exo* in character, of the $(M_3)_2$ subunit now overlap with the AOs of the interstitial N atom into four bonding a_{1g}, a_{2u} and e_u MOs (D_{3d} symmetry). Saturated d orbitals of the late transition metal do not participate in bonding. The skeletal electron count for an inverted pair is then equal to $(2\times 62)-8=132$.

3.4. Relation to the extended icosahedral structures

As the term icosogen has been used by King [183] to characterize Group 13 elements, it is not surprising that the stable icosahedral cluster is the most frequent building block occurring within anionic cluster frameworks. The M_{12} icosahedra are connected together, mostly by (2c–2e) bonds between vertices of adjacent units. Whereas icosahedral symmetry can propagate in long range or aperiodic structures (quasi-crystals) provided that some lattice distortions occur, in periodic 3D networks pseudo-extended icosahedral structures may be observed, but within the boundary of a few shells around an "icosahedral core".

In the cubic $Im\bar{3}$ phase $Li_{13}Cu_6Ga_{21}$ [184], low-coordinated and isolated atoms are no longer found. Starting from the (0, 0, 0) position, 12 Ga atoms form an icosahedron (shaded in Fig. 23), and 20 Li atoms radiate from the centres of its 20 triangular faces forming the dual pentagonal dodecahedron. 12 Cu atoms out of centres of the pentagonal faces of the dodecahedron are 2c–2e connected to the central icosahedron and cap the 12 pentagonal faces of a fullerene-like Ga_{60} truncated

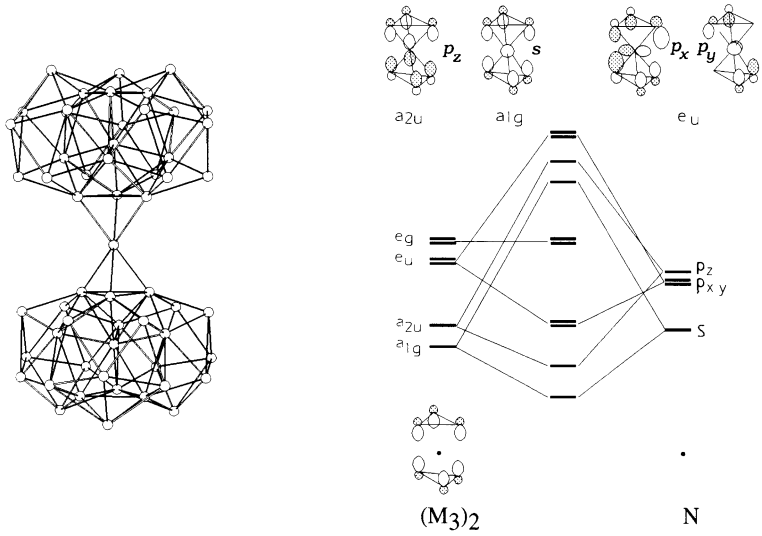

Fig. 22. Bonding scheme around the central N atom within the $M_{28}NM_{28}$ cluster (D_{3d}).

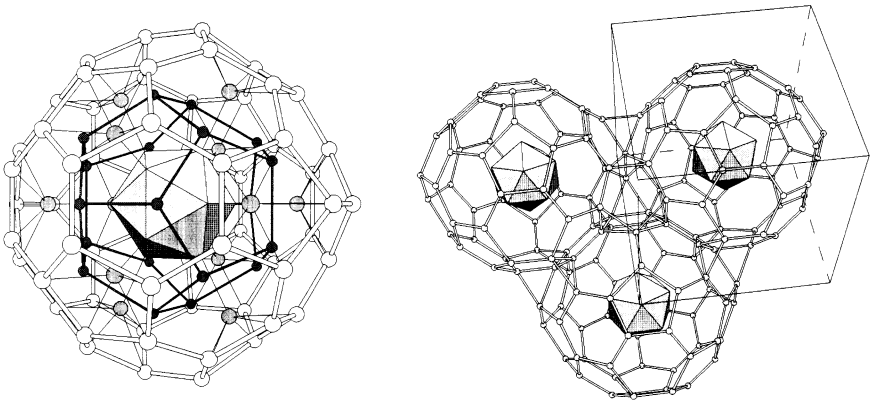

Fig. 23. Extension of the pseudo five-fold symmetry from icosahedron to Samson's polyhedron (left) and polyhedral packing within the $Li_{13}Cu_6Ga_{21}$ $Im\bar{3}$ cubic cell (right).

icosahedron from the inside. Li and Cu atoms are arranged on a (30 rhombic faces) triacontahedron. These successive onion-like layers of electronegative and electropositive elements form the 104-atom polyhedron which can be formulated as $Ga_{12}@Li_{20}@Cu_{12}@Ga_{60}$ according to an endohedral formalism.

Similar units are found in the isostructural r-Li_3CuAl_5 phase. This phase may be prepared from a melt of composition $Al_{59}Cu_{10.5}Li_{30.5}$, and forms a "duplex" structure in which it is surrounded by a continuous layer of the i-Li_3CuAl_6 quasi-crystalline phase [185]. Transmission electron microscopy provides evidence for a close orientation relationship between the two phases, such that the r-Li_3CuAl_5 phase has been referred to as a quasi-crystal approximant. The 104-atom polyhedron is the unique repeating unit in the bcc $Li_{13}Cu_6Ga_{21}$ structure. Packing along {111} and along {100} involves hexagonal face-sharing and edge-sharing, respectively. Here, pseudo five-fold symmetry propagation is limited to a few shells. In contrast, in YB_{66} [186], the range of propagation is slightly longer since an icosahedron is surrounded by 12 icosahedra but within a boundary imposed by the presence of disordered low-coordinated boron atoms.

A Samson polyhedron exists in some cfc structures such as $Na_{35}Cd_{24}Ga_{56}$, $Na_{36}Ag_7Ga_{73}$, $Li_{18}Cu_5In_4Ga_{31}$ (see Table 3, Fig. 24). In these structures the icosahedron is bonded to six icosahedra and to six 16-atom icosioctahedra (28 triangular faces). The latter can be considered as a tetracapped truncated tetrahedron, and thus has tetrahedral symmetry. The icosioctahedron has 36 skeletal electrons, two more than Wade's requirement for a *closo* cluster. Successive coordination shells form a 145-atom polyhedron, formulated as $A@M_{16}@A_{28}@M_{16}@M_{84}$ (A = alkali metal cation), with tetrahedral symmetry (see Fig. 25). The A_{28} hexadecahedron has 12 pentagonal and four hexagonal faces and the outer M_{84} shell 12 pentagonal and 32 hexagonal faces. In these cfc structures, icosahedron-centred 104-atom and icosioctahedron-centred 145-atom polyhedra interpenetrate.

Table 3
Principal features of phases hierarchically related to the C15 structural type

Compound	Reference	α	Mean charge per heavy atom	Anionic network description
Na_7Ga_{13}	[157,158]	57.36	−0.538	Ga_{12}, Ga_{15}
$K_{21.33}In_{39.67}$	[187]	57.53	−0.538	In_{12}, In_{15}
$Na_{12}K_{18}In_{53}Tl_7$	[188]	57.85	−0.504	$(In/Tl)_{12}$, $(In/Tl)_{16}$
$Na_{35}Cd_{24}Ga_{56}$	[176]	60	−0.438	Ga_{12}, $Cd_{12}Ga_4$
$Na_{36}Ag_7Ga_{73}$	[177]	60	−0.450	Ga_{12}, Ag_4Ga_{12}
$Li_{18}Cu_5In_4Ga_{31}$	[178]	60	−0.450	$(Cu/Ga)_{12}$, In_4Ga_{12}
$Na_{17}Ga_{29}In_{12}$	[189]	60	−0.415	In_{12}, $In_{12}Ga_5$
$K_{17}In_{41}$	[189]	60	−0.415	In_{12}, In_{17}
$Na_{13}K_4Ga_{47.45}$	[170,171]	65.77	−0.358	Ga_{12}, Ga_{28}
$Na_{21}K_{14}Cd_{17}Ga_{82}$	[172]	65.03	−0.354	$(Ga/Cd)_{12}$, $(Ga/Cd)_{28}$
$Na_{102}Cu_{36}Ga_{279}$	[173]	65.30	−0.324	$(Ga/Cu)_{12}$, $\{Cu,2(Ga/Cu)_{28}\}$
$Na_{102}Zn_{72}Ga_{243}$	[174]	65.72	−0.324	$(Ga/Zn)_{12}$, $\{Zn,2(Ga/Zn)_{28}\}$
$Na_{34}Cu_6Cd_7Ga_{92}$	[175]	65.54	−0.324	Ga_{12}, $(Ga/Cd)_{12}$, $\{Cu,2(Ga_{25}Cu_3)\}$
$K_{34}Zn_{20}In_{85}$	[190]	65.24	−0.324	In_{12}, $Zn_{10}In_{18}$

α = angle of the primitive rhombohedral cell;
α = 60° for *Fd3m* structures, α ≠ 60° for $R\bar{3}m$ structures.

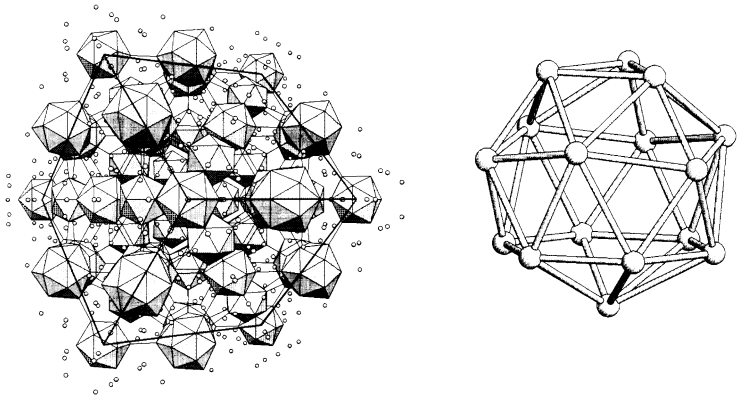

Fig. 24. Packing within the *Fd3m* $Li_{18}Cu_5In_4Ga_{31}$ compound (left). The 16-atom, 28-faces icosioctahedron (right).

An outer M_{84} coordination shell (12 pentagonal and 32 hexagonal faces) with hexagonal symmetry has been found in the quaternary compound $Na_8K_{23}Cd_{12}In_{48}$ [188] and contains a $Cd_{12}In_6$ tube-like cluster. This tubular cluster encloses two alkali metal cations and is surrounded by a 32-alkali metal cation cage. Cd atoms at the top and bottom of the $Cd_{12}In_6$ triple-decker are 2c–2e *exo* bonded to six In_{12} icosahedra while In atoms are not *exo* bonded. 12-Coordination of the icosahedron is achieved via triangular In_3 fragments (−1 oxidation state for In) (Figs. 25 and 26).

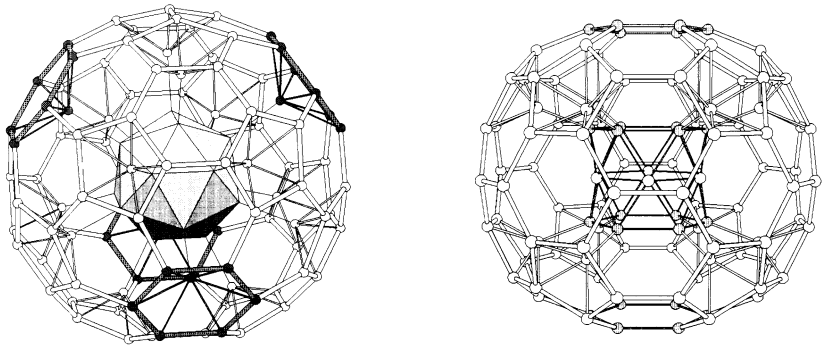

Fig. 25. M_{84} outer coordination shells around tetrahedral icosioctahedron (left) and hexagonal $Cd_{12}In_6$ (right) cluster.

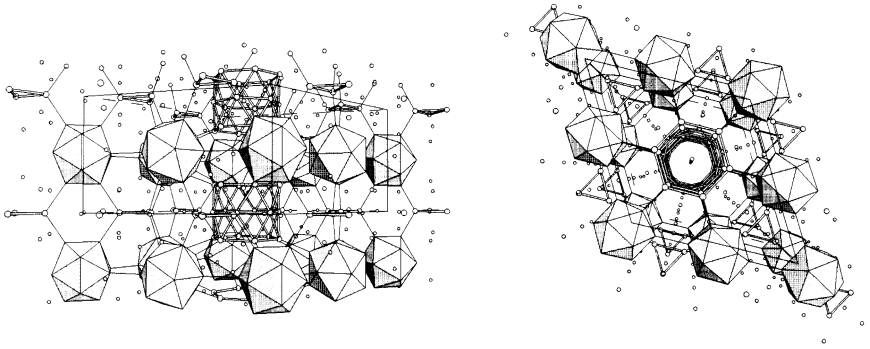

Fig. 26. Two views of the hexagonal *P6/mmm* $Na_8K_{23}Cd_{12}In_{48}$ structure.

A VEC of 68 (PEC = 80) for the $Cd_{12}In_6$ cluster has been obtained from EHMO calculations. Assuming that a VEC of 38 still holds for the icosahedron, the anionic formulation $3In_{12}^{2-}$, $2In_3^{3-}$, $Cd_{12}In_6^{26-}$ leads to a number of electrons that exceeds by seven the number of valence electrons ($199e^-$) actually supplied by the atoms (including alkali metals) in a formula unit. The open shell nature of this compound is clearly demonstrated by the band structure (Fig. 27) in which the Fermi level ($199e^-$) cuts several bands in agreement with the metallic character shown by resistivity measurements. With 206 electrons, $Na_8K_{23}Cd_{12}In_{48}$ would have a closed shell and be a semiconductor. This has raised the question of knowing where the seven additional electrons would be located if the compound could be further reduced. Density of states (DOS) curves indicate that the $Cd_{12}In_6$ cluster, which is the only contributor to bands near the actual Fermi level, is the potential electron-acceptor [188]. Analysis of crystal orbital overlap populations (COOP, which indicate the bonding, non-bonding or antibonding nature of levels in a certain energy range) shows that the additional electrons would fill levels which bond at In–In edges of the $Cd_{12}In_6$ cluster.

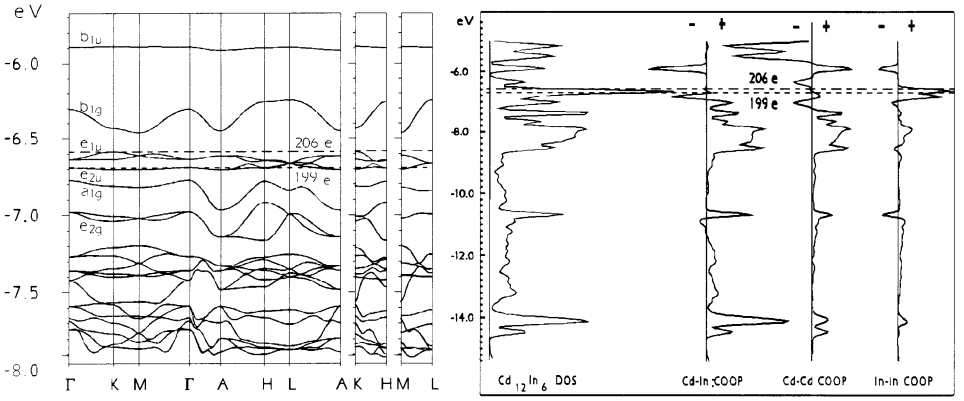

Fig. 27. Dispersion curves, partial DOS and COOP for $Cd_{12}In_6$ tube-like cluster in $Na_8K_{23}Cd_{12}In_{48}$.

3.5. Hierarchical relation to the C15 ($MgCu_2$) family

Selected features of anionic networks in some alkali metal–early post-transition element phases, hierarchically related to the C15 Friauf–Laves structure type ($MgCu_2$), are summarized in Table 3. All these phases can be described in their primitive rhombohedral cell with α equal to 60° for the cubic *Fd*$\bar{3}$*m*, but differing slightly from 60° for the *R*$\bar{3}$*m* phases. In all these structures, the centres of the icosahedra are arranged on a Kagomé network at the position of the copper atoms in the $MgCu_2$ structure type, the Mg sites being occupied by other polyhedra. The electron-richer ones have been referred to as "spacers". These polyhedra are the mostly electron-precise M_{15} or M_{16} open spacers [Fig. 29(b, c) later] present in moderately reduced rhombohedral phases (top of Table 3), the regular (deltahedral) M_{16} icosioctahedron [Fig. 29(d)] in cubic phases and the electron-poor tri-icosahedron [Fig. 29(a)] in less reduced rhombohedral phases (bottom of Table 3). Using actual symmetries, these polyhedra are connected to identical units in different bonding patterns. In cubic phases, the icosioctahedron is tetrahedrally connected to four icosioctahedra by 2c–2e bonds. An open M_{15} spacer in *R*$\bar{3}$*m* phases is bonded around the three-fold axis to three like units (through double connections), but is not interconnected along the ternary axis as is the M_{16} spacer (Fig. 28).

Similarly, the triply-fused icosahedron is not interconnected along the three-fold axis in *R*$\bar{3}$*m* $Na_{13}K_4Ga_{47.45}$ and forms an inverted unit ($M_{28}NM_{28}$) in $Na_{17}Cu_6Ga_{46.5}$ and $Na_{17}Zn_{12}Ga_{40.5}$ with a coordinating heteroatom at the $\bar{3}m$ centre (see Figs. 21 and 22). The wide (but flattened) triply-fused icosahedron more efficiently fills voids between icosahedra allowing full *exo* bonding of icosahedron at site 3(b), which is only six-fold *exo* bonded in rhombohedral structures containing the open M_{15} and M_{16} spacers. For less reduced networks containing triply-fused icosahedra, the smaller number of solvating alkali metal cations is responsible for the contraction of the rhombohedral cells ($\alpha > 60°$) along the three-fold axis. In

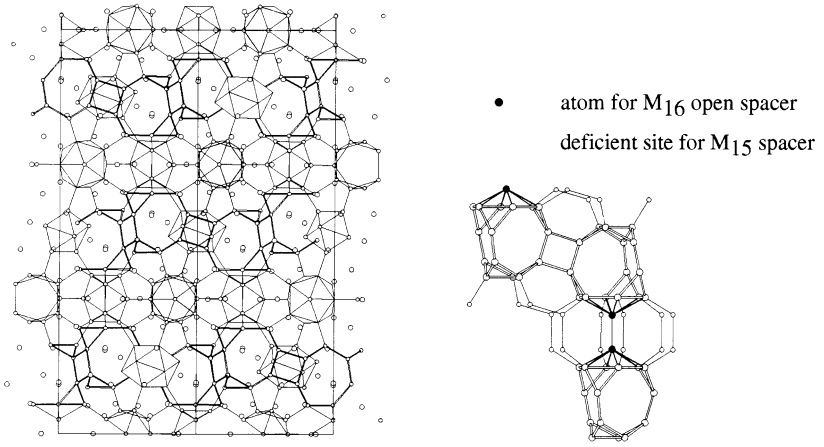

Fig. 28. Projection of crystal structure of $R\bar{3}m$ $Na_{12}K_{18}In_{53}Tl_7$ and viewing of spacers (M_{16} in $Na_{12}K_{18}In_{53}Tl_7$ and M_{15} in $Na_{22}Ga_{39}$) interconnections.

contrast, the rhombohedral cells are elongated ($\alpha < 60^\circ$) for more reduced networks, including more alkali metal cations.

Previous calculations have shown the doubly-*nido* or triply-*nido* tri-icosahedra to be stabilized with 62 skeletal electrons, the open M_{15} and M_{16} polyhedra with 44 and the regular M_{16} icosioctahedron with 36 skeletal electrons. There are striking correlations not only between phases discussed above, but also with other phases which cannot be derived so simply from the C15 structural family. However, the "electronic surgery" which would transform the electron-deficient tri-icosahedron into electron-richer spacers (Fig. 29) still remains obscure.

Reduction (removal of the three top atoms) of the 36 skeletal electron-centred icosioctahedron [Fig. 29(d)] would give the 32 skeletal electron collapsed M_{14} cluster [Fig. 29(e)] as recently found in $K_{49}Tl_{108}$ [191]. Further reduction (removal of the cap and central atoms) leads to the more classical hexagonal antiprismatic M_{12} cluster [30 skeletal electrons, Fig. 29(f)] as found in $A_3Na_{26}In_{48}$ (A = K, Rb, Cs) [192,193]. Finally, condensation of two M_{12} clusters would give the triple-decker M_{18} represented by the $Cd_{12}In_6$ tubular cluster recently found in the $Na_8K_{23}Cd_{12}In_{48}$ hexagonal phase [188].

3.6. Isolated or naked clusters of Group 13 elements

Indium and particularly thallium are very prolific in isolated anions. Owing to the paucity of electrons of the elements, anions are considered with high formal charges. These should not be taken as real charges, as strong interactions with solvating alkali metals are likely to draw back electron density to the polarizing cations. Anyway, these formal charges are useful to rationalize structures and estimate electron counts.

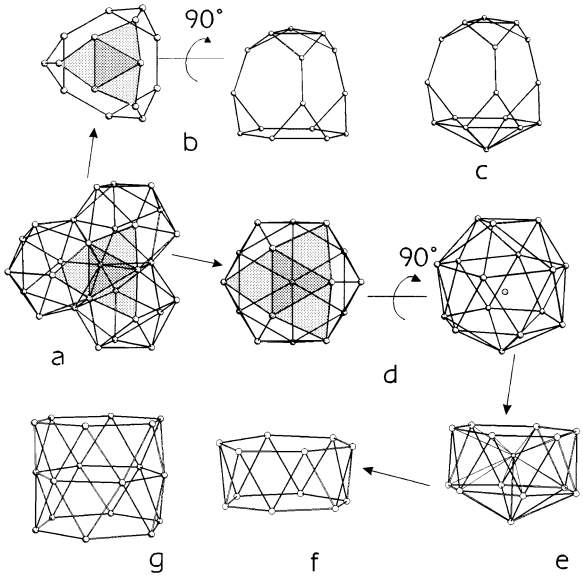

Fig. 29. Some network polyhedra and spacers: (a) triply-fused icosahedron; (b) M_{15} open polyhedron; (c) M_{16} open polyhedron; (d) icosioctahedron; (e) M_{14} collapsed polyhedron; (f) hexagonal M_{12} antiprism; (g) triple-decker M_{18} polyhedron.

Clusters can be categorized into two groups.

- Relatively small sized clusters such as tetrahedral In_4^{8-} and Tl_4^{8-} (12 SEs, skeletal electrons) better described with electron-precise bonding and others which conform to Wade's rules as *closo* Tl_5^{7-} (12 SEs), *nido* In_5^{9-} (14 SEs), and *closo* Tl_6^{8-} (14 SEs).
- Fairly large clusters which are hypoelectronic with regard to Wade's rules such as In_{11}^{7-}, Tl_{11}^{7-} (18 SEs), $Tl_9Au_2^{9-}$ (16 SEs), Tl_6^{6-} (12 SEs), Tl_9^{9-} (18 SEs) and centred (18 SEs) $In_{10}Zn^{8-}$, $Tl_{10}Zn^{8-}$ and $In_{10}M^{10-}$ (M = Ni, Pd, Pt) [194].

Centring of clusters is a means to stabilize hypoelectronic clusters, interstitial atom s- and p-orbitals overlap with the MOs of the empty cluster in order to decrease the total energy. Furthermore, use of an electron-donor centring element reduces the anionic charge. This can be exemplified with the icosahedral $Tl_{12}M^{12-}$ (M = Mg, Zn, Cd, Hg) which satisfies Wade's requirement for a *closo* cluster (PEC = 50). $Tl_{12}Na^{13-}$ and Tl_{13}^{11-} are isoelectronic analogues.

The $Tl_{12}Cd^{12-}$ cluster, present in the compound $K_6(NaCd)_2Tl_{12}Cd$ [195], has been considered as "not so naked" owing to interactions with neighbouring icosahedra through four cadmium atoms which substitute at 50% for sodium atoms capping (in the first solvation shell) eight of the icosahedron faces (Fig. 30). Band calculations clearly show the covalent nature of this antiprismatic Cd bridging, somewhat featuring interactions which may generally occur between clusters and polarizing solvating alkali metal cations. In the $K_6(NaCd)_2Tl_{12}Cd$, closed-shell and

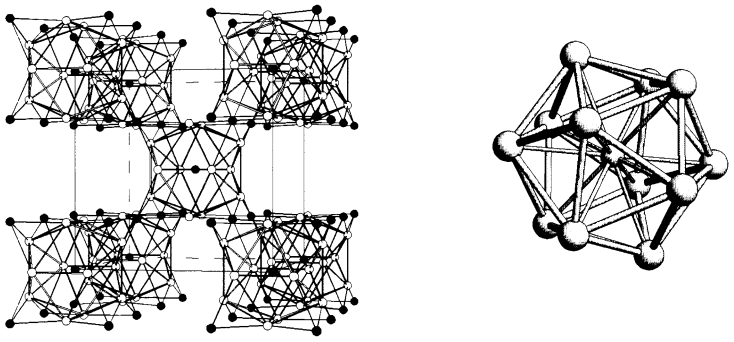

Fig. 30. Crystal structure of $Im\bar{3}$ $K_6(NaCd)_2Tl_{12}Cd$ and the Cd-centred Tl_{12} cluster.

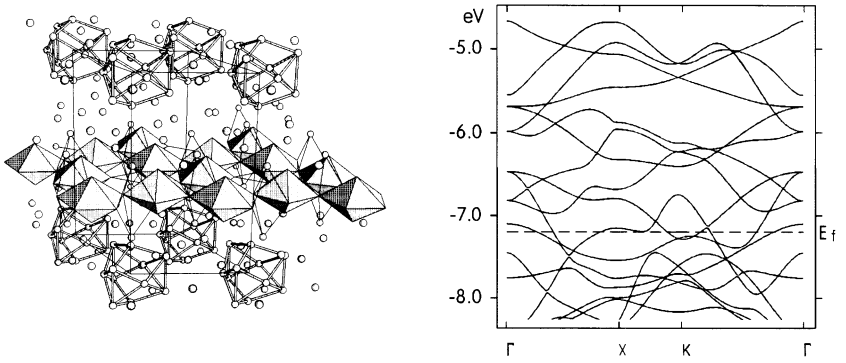

Fig. 31. The $K_{14}Cd_9Tl_{21}$ ($P\bar{6}m2$) hexagonal compound and 2-D band structure of the $Cd_9Tl_{10}^{7-}$ slab.

semiconducting compound, the polyhedral count for $Tl_{12}Cd^{12-}$ remains unchanged (50 electrons).

3.7. Intermediate cluster frameworks

There can be some intermediate phases where naked clusters coexist with cluster frameworks. There are two interesting hexagonal structures for such compounds: $A_{15}Tl_{27}$ (A = Rb, Cs) [196] containing layers of naked Tl_{11}^{7-} anions which alternate with a $^2_\infty[Tl_{16}^{8-}]$ network built from the condensation of Tl_{11} units and $K_{14}Cd_9Tl_{21}$ [197] in which the Tl_{11}^{7-} layers are associated with a $^2_\infty[Cd_9Tl_{10}^{7-}]$ slab. This slab would be better described with condensed pentagonal Cd_5Tl_2 bipyramids with each trimeric unit capped, on the three-fold axis, by two additional Tl atoms. The hypoelectronic nature of the Tl_{11}^{7-} (18 skeletal electrons) has been confirmed. The 3D band structure [198] clearly shows, at least within the context of the extended Hückel method, that the K–Tl interactions are very weak and there is no appreciable electronic transfer between Tl_{11}^{7-} anions and the $Cd_9Tl_{10}^{7-}$ slab. 2D calculations also

indicate that bonding within such layers is highly delocalized, providing metallic properties to the material (Fig. 31).

Acknowledgements

The authors are indebted to a group of coworkers for their contributions to some of the work described in this paper and D. Jones for checking the final english version. This research has been supported by the ''Ministère de l'Education Nationale'' and the ''Centre National de la Recherche Scientifique''.

References

[1] F. Laves, Theory of Alloys Phases, American Society of Metals, Cleveland, OH, 1956, p. 124.
[2] W. Hume-Rothery, J. Inst. Met. 35 (1926) 309.
[3] W.B. Pearson, J. Less Common Met. 100 (1984) 229.
[4] W.B. Pearson, J. Less Common Met. 109 (1985) L3.
[5] J.B. Friauf, J. Am. Chem. Soc. 49 (1927) 3107.
[6] L. Pauling, J. Solid State Chem. 54 (1984) 297.
[7] L. Pauling, Z.S. Herman, in: Z.B. Maksic (Ed.), Modelling of Structures and Properties of Molecules, Ellis Horwood, Chichester, UK, 1987, p. 5.
[8] E. Zintl, J. Goubeau, W. Dullenkopf, J. Phys. Chem. A 154 (1931) 1.
[9] E. Zintl, A. Harder, J. Phys. Chem. A 154 (1931) 47.
[10] E. Zintl, W. Dullenkopf, Z. Phys. Chem. B 16 (1932) 195.
[11] E. Zintl, H. Kaiser, Z. Anorg. Allg. Chem. 211 (1933) 113.
[12] E. Zintl, G. Brauer, Z. Phys. Chem. B 20 (3/4) (1933) 245.
[13] J. Witte, H.G. von Schnering, Z. Anorg. Allg. Chem. 327 (1964) 260.
[14] I. Böhm, O. Hassel, Z. Anorg. Allg. Chem. 160 (1927) 152.
[15] K.H. Janzon, H. Schäfer, A. Weiss, Z. Naturforsch. 23b (1968) 1544.
[16] G. Nagorsen, H. Posch, H. Schäfer, A. Weiss, Z. Naturforsch. 24b (1969) 1191.
[17] A. Iandelli, Rend. Acc. Naz. Lincei 19 (1955) 307.
[18] W. Klemm, E. Busmann, Z. Anorg. Allg. Chem. 319 (1963) 297.
[19] W. Müller, J. Stöhr, Z. Naturforsch. 32b (1977) 631.
[20] K. Deller, B. Eisenmann, Z. Anorg. Allg. Chem. 425 (1976) 104.
[21] K. Deller, B. Eisenmann, Z. Naturforsch. 31b (1976) 1146.
[22] V.J. Stöhr, H. Schäfer, Z. Anorg. Allg. Chem. 474 (1981) 221.
[23] M. Tillard-Charbonnel, C. Belin, C.R. Acad. Sci. Paris, Série II 306 (1988) 1161.
[24] M. Tillard-Charbonnel, C. Belin, J.L. Soubeyroux, Eur. J. Solid State Inorg. Chem. 27 (1990) 759.
[25] C.R. Eady, B.F.G. Johnson, J. Lewis, B.E. Reichert, G.M. Sheldrick, J. Chem. Soc., Chem. Commun. (1976) 271.
[26] J.C. Calabrese, L.F. Dahl, A. Cavalieri, P. Chini, G. Longoni, S. Martinengo, J. Am. Chem. Soc. 96 (1974) 2616.
[27] C.E. Briant, B.R.C. Theobald, J.W. White, L.K. Bell, D.M.P. Mingos, A.J. Welch, J. Chem. Soc., Chem. Commun. (1981) 201.
[28] E.L. Muetterties, Special reports, C&EN 30 (1982) 28.
[29] P. Braunstein, J. Rose, in: E.W. Abel, F.G.A. Stone, G. Wilkinson (Eds.), Comprehensive Organometallic Chemistry, 2nd ed., vol. 10, Pergamon, Oxford, 1995, ch. 7, pp. 351–385.
[30] P. Braunstein, J. Rose, in: R.D. Adams, F.A. Cotton (Eds.), Catalysis by Di- and Polynuclear Metal Clusters, Wiley, New York, 1997, pp. 346–402.
[31] P. Chini, J. Organomet. Chem. 200 (1981) 37.

[32] B.F.G. Johnson, J. Lewis, Adv. Inorg. Chem. Radiochem. 24 (1981) 225.
[33] F.G.A. Stone, Angew. Chem. Int. Ed. Engl. 23 (1984) 89.
[34] H. Vahrenkamp, Adv. Organomet. Chem. 22 (1983) 169.
[35] E. Sappa, A. Tiripicchio, P. Braunstein, Chem. Rev. 83 (1983) 203.
[36] A. Simon, Angew. Chem. Int. Ed. Engl. 27 (1988) 159.
[37] J.D. Corbett, Acc. Chem. Res. 14 (1986) 239.
[38] R. Chevrel, M. Sergent, J. Prigent, J. Solid State Chem. 3 (1971) 315.
[39] A. Simon, Struct. Bond. 36 (1977) 81.
[40] A. Simon, Angew. Chem. Int. Ed. Engl. 27 (1988) 159.
[41] R.J. Gillespie, J. Passmore, Adv. Inorg. Chem. Radiochem. 17 (1975) 49.
[42] G. Gnutzmann, F.W. Dorn, W. Klemm, Z. Anorg. Allg. Chem. 309 (1961) 210.
[43] J. Roziere, A. Seigneurin, C. Belin, A. Michalowicz, Inorg. Chem. 24 (1985) 3710.
[44] J.D. Corbett, Inorg. Chem. 7 (1968) 198.
[45] R.C. Burns, R.J. Gillespie, W.C. Luk, Inorg. Chem. 17 (1978) 3596.
[46] S. Ulvenlund, K. Stahl, L. Bengtsson-Kloo, Inorg. Chem. 35 (1996) 223.
[47] N.J. Bjerrum, G.P. Smith, Inorg. Chem. 6 (1967) 1968.
[48] R.M. Friedman, J.D. Corbett, Inorg. Chem. 12 (5) (1973) 1134.
[49] M.J. Collins, R.J. Gillespie, J.F. Sawyer, Inorg. Chem. 26 (1987) 1476.
[50] A. Manteghetti, J. Roziere, A. Seigneurin, J. Chem. Soc., Faraday Trans. 86 (9) (1990) 1579.
[51] R.C. Burns, R.J. Gillespie, W.C. Luk, D.R. Slim, Inorg. Chem. 18 (1979) 3086.
[52] R.J. Gillespie, W.C. Luk, D.R. Slim, J. Am. Chem. Soc. 844 (1976) 791.
[53] A. Cisar, J.D. Corbett, Inorg. Chem. 16 (1977) 2482.
[54] R.G. Teller, L.J. Krause, R.C. Haushalter, Inorg. Chem. 22 (1983) 1809.
[55] A. Cisar, J.D. Corbett, Inorg. Chem. 16 (1977) 632.
[56] H.G. von Schnering, Angew. Chem. Int. Ed. Engl. 20 (1981) 33.
[57] W. Schmettow, H.G. von Schnering, Angew. Chem. Int. Ed. Engl. 16 (1977) 857.
[58] H.G. von Schnering, W. Hönle, Chem. Rev. 88 (1988) 243.
[59] J.F. Smith, A. Hansen, Acta Crystallogr. 22 (1967) 836.
[60] J.D. Corbett, in: S. Kauzlarich (Ed.), Chemistry, Structure and Bonding of Zintl Phases and Ions, VCH, New York, 1996, ch. 3.
[61] G. Cordier, V. Müller, Z. Krist. 198 (1992) 281.
[62] G. Cordier, V. Müller, Z. Naturforsch. 49b (1994) 935.
[63] A. Johannis, C.R. Hebd. Sceances Acad. Sci. 113 (1891) 795.
[64] A. Johannis, C.R. Hebd. Sceances Acad. Sci. 114 (1892) 587.
[65] C.A. Kraus, J. Am. Chem. Soc. 29 (1907) 1571.
[66] F.H. Smyth, J. Am. Chem. Soc. 39 (1917) 1299.
[67] C.A. Kraus, J. Am. Chem. Soc. 44 (1922) 1216.
[68] C.A. Kraus, Trans. Am. Electrochem. Soc. 45 (1924) 175.
[69] D. Kummer, L. Diehl, Angew. Chem. Int. Ed. Engl. 9 (1970) 895.
[70] L. Diehl, K. Khodadedeh, D. Kummer, J. Strähle, Z. Naturforsch. 31b (1976) 522.
[71] L. Diehl, K. Khodadedeh, D. Kummer, J. Strähle, J. Chem. Ber. 109 (1976) 3404.
[72] J.D. Corbett, P.A. Edwards, J. Am. Chem. Soc. 99 (1977) 3313.
[73] J.M. Lehn, Struct. Bond. Berlin 16 (1973) 1.
[74] J. Campbell, G.J. Schrobilgen, Inorg. Chem. 36 (1997) 4078.
[75] C.H.E. Belin, J.D. Corbett, A. Cisar, J. Am. Chem. Soc. 99 (1977) 7163.
[76] V. Angillella, C. Belin, J. Chem. Soc., Faraday Trans. 87 (1) (1991) 203.
[77] T.F. Fässler, M. Hunziker, Inorg. Chem. 33 (1994) 5380.
[78] C. Belin, H. Mercier, V. Angillella, New J. Chem. 15 (1991) 931.
[79] P.A. Edwards, J.D. Corbett, Inorg. Chem. 16 (1977) 903.
[80] J. Campbell, D.A. Dixon, H.P.A. Mercier, G.J. Schrobilgen, Inorg. Chem. 34 (1995) 5798.
[81] S.C. Critchlow, J.D. Corbett, J. Am. Chem. Soc. 105 (1983) 5715.
[82] S.C. Critchlow, J.D. Corbett, Inorg. Chem. 23 (1984) 770.
[83] A. Cisar, J.D. Corbett, Inorg. Chem. 16 (1977) 2482.
[84] U. Bolle, W. Tremel, J. Chem. Soc., Chem. Commun. 2 (1992) 91.

[85] C. Belin, H. Mercier, B. Bonnet, B. Mula, C.R. Acad. Sci. Paris 307 (1988) 549.
[86] C.H.E. Belin, J. Am. Chem. Soc. 102 (1980) 6036.
[87] R.C. Haushalter, J. Chem. Soc., Chem. Commun. (1987) 196.
[88] S.C. Critchlow, J.D. Corbett, Inorg. Chem. 24 (1985) 979.
[89] R.C. Burns, J.D. Corbett, J. Am. Chem. Soc. 103 (1981) 2627.
[90] R.C. Burns, J.D. Corbett, J. Am. Chem. Soc. 104 (1982) 2804.
[91] C.H.E. Belin, M.M. Charbonnel, Inorg. Chem. 21 (1982) 2504.
[92] C.H.E. Belin, C.R. Acad. Sci. Paris, Série II 298 (16) (1984) 691.
[93] C.H.E. Belin, H.P.A. Mercier, J. Chem. Soc., Chem. Commun. (1987) 191.
[94] M. Björgvinsson, J.F. Sawyer, G.J. Schrobilgen, Inorg. Chem. 30 (1991) 2231.
[95] M. Björgvinsson, J.F. Sawyer, G.J. Schrobilgen, Inorg. Chem. 26 (1987) 741.
[96] D.M. Smith, C.W. Park, J.A. Ibers, Inorg. Chem. 35 (1996) 6682.
[97] C.H. Belin, V.E. Angillella, H.P. Mercier, Acta Crystallogr. C 47 (1991) 61.
[98] J. Campbell, D.P. DiCiommo, H.P.A. Mercier, A.M. Pirani, G.J. Schrobilgen, M. Willuhn, Inorg. Chem. 34 (1995) 6265.
[99] M. Ansari, J. Ibers, S. O'Neal, W. Pennington, J. Kolis, Polyhedron 11 (15) (1992) 1877.
[100] V. Angillella, H. Mercier, C. Belin, J. Chem. Soc., Chem. Commun. (1989) 1655.
[101] H.P. Mercier, V.E. Angillella, C.H. Belin, New J. Chem. 14 (1990) 121.
[102] C.J. Warren, D.M. Ho, R.C. Haushalter, A.B. Bocarsly, Angew. Chem. Int. Ed. Engl. 32 (11) (1993) 1646.
[103] C.J. Warren, S.S. Dhingra, D.M. Ho, R.C. Haushalter, A.B. Bocarsly, Inorg. Chem. 33 (1994) 2709.
[104] S. Sportouch, J. Thumim, M. Tillard-Charbonnel, C. Belin, New J. Chem. 19 (1995) 133.
[105] J.W. Kolis, Phosphorus, Sulfur, Silicon Relat. Comp. 93 (1994) 93.
[106] C.W. Park, M.A. Pell, J.A. Ibers, Inorg. Chem. 35 (1996) 4555.
[107] H.C. Longuet-Higgins, M. de V. Roberts, Proc. R. Soc. London, Ser. A 224 (1954) 336.
[108] H.C. Longuet-Higgins, M. de V. Roberts, Proc. R. Soc. A 230 (1955) 110.
[109] W.N. Lipscomb, Boron Hydrides, Benjamin, New York, 1963.
[110] B.K. Teo, Inorg. Chem. 23 (1984) 1251.
[111] B.K. Teo, Inorg. Chem. 23 (1984) 1627.
[112] B.K. Teo, Inorg. Chem. 24 (1985) 4209.
[113] B.K. Teo, Polyhedron 9 (15/16) (1990) 1985.
[114] B.K. Teo, G. Longoni, F.R.K. Chung, Inorg. Chem. 23 (1984) 1257.
[115] R. Mason, K.M. Thomas, D.M.P. Mingos, J. Am. Chem. Soc. 95 (1973) 3802.
[116] K. Wade, J. Chem. Soc., Chem. Commun. (1971) 792.
[117] K. Wade, Adv. Inorg. Chem. Radiochem. 18 (1976) 1.
[118] D.M.P. Mingos, Nature (Phys. Sci.) 236 (1972) 99.
[119] D.M.P. Mingos, D.J. Wales, Introduction to Cluster Chemistry, Prentice-Hall, Englewood Cliffs, NJ, 1990.
[120] R.E. Williams, Inorg. Chem. 10 (1971) 210.
[121] R.W. Rudolph, Acc. Chem. Res. 9 (1976) 446.
[122] D.M.P. Mingos, Acc. Chem. Res. 17 (1984) 311.
[123] L. Guggenberger, Inorg. Chem. 7 (1968) 2260.
[124] J.D. Corbett, Chem. Rev. 85 (1985) 383.
[125] R.D. Dobrott, W.M. Lipscomb, J. Chem. Phys. 37 (1962) 1779.
[126] B. Schiemenz, G. Huttner, Angew. Chem. Int. Ed. Engl. 32 (1993) 297.
[127] B.W. Eichhorn, R.C. Haushalter, W.T. Pennington, J. Chem. Soc., Chem. Commun. (1990) 937.
[128] B.W. Eichhorn, R.C. Haushalter, J. Am. Chem. Soc. 110 (1988) 8704.
[129] T.J. Bastow, H.J. Whitfield, J. Chem. Soc., Dalton Trans. (1973) 1739.
[130] H.J. Whitfield, J. Chem. Soc., Dalton Trans. (1973) 1740.
[131] H.J. Whitfield, J. Chem. Soc., Dalton Trans. (1973) 1737.
[132] W.S. Sheldrick, Z. Naturforsch. 43b (1988) 249.
[133] T.M. Martin, P.T. Wood, J.W. Kolis, Inorg. Chem. 33 (1994) 1587.
[134] B.W. Eichhorn, R.C. Haushalter, J.C. Huffmann, Angew. Chem. Int. Ed. Engl. 28 (8) (1989) 1032.

[135] G. Fritz, K.D. Hoppe, W. Hönle, D. Weber, C. Mujica, V. Manriquez, H.G. von Schnering, J. Organomet. Chem. 249 (1983) 63.
[136] S. Sportouch, M. Tillard-Charbonnel, C. Belin, J. Chem. Soc., Dalton Trans. (1995) 3113.
[137] L.R. Sita, I. Kinoshita, Organometallics 9 (1990) 2865.
[138] P. Boldrini, I.D. Brown, M.J. Collins, R.J. Gillespie, E. Maharajh, D.R. Slim, J.F. Sawyer, Inorg. Chem. 24 (1985) 4302.
[139] R.C. Burns, R.J. Gillespie, Inorg. Chem. 21 (1982) 3877.
[140] J. Beck, Z. Naturforsch. 45b (4) (1993) 413.
[141] F.U. Axe, D.S. Marynick, Inorg. Chem. 27 (1988) 1426.
[142] R.J. Cave, E.R. Davidson, P. Sauter, E. Canadell, O. Eisenstein, J. Am. Chem. Soc. 111 (1989) 8105.
[143] B. Eisenmann, K.H. Janzon, H. Schäfer, A. Weiss, Z. Naturforsch. 24b (1969) 457.
[144] P. Böttcher, Angew. Chem. Int. Ed. Engl. 27 (1988) 759.
[145] J. Beck, Angew. Chem. Int. Ed. Engl. 33 (1994) 163 and references cited therein
[146] H.G. von Schnering, R. Nesper, Acta Chem. Scand. 45 (1991) 870.
[147] C. Belin, Acta Crystallogr. B 37 (1981) 2060.
[148] R.E. Marsh, F.H. Herbstein, Acta Crystallogr. B 39 (1983) 280.
[149] J.H.N. Van Vucht, J. Less Common Met. 108 (1985) 163.
[150] C. Belin, R.G. Ling, C.R. Acad. Sci. Paris 480 (1982) 181.
[151] S.P. Yatsenko, E.I. Gladyshevskii, K.A. Chuntonov, Ya.P. Yarmoluk, Yu.N. Grin, Sov. Phys. Crystallogr. 28 (4) (1983) 479.
[152] R.G. Ling, C. Belin, Z. Anorg. Allg. Chem. 480 (1981) 181.
[153] J.H.N. Van Vucht, J. Less Common Met. 108 (1985) 163.
[154] S.C. Sevov, J.D. Corbett, Z. Anorg. Allg. Chem. 619 (1993) 128.
[155] C. Belin, Acta Crystallogr. B 36 (1980) 1339.
[156] C. Belin, M. Tillard-Charbonnel, Prog. Solid State Chem. 22 (1993) 59.
[157] U. Frank-Cordier, G. Frank-Cordier, H. Schäfer, Z. Naturforsch. 37b (1982) 119.
[158] U. Frank-Cordier, G. Frank-Cordier, H. Schäfer, Z. Naturforsch. 37b (1982) 127.
[159] R.G. Ling, C. Belin, Acta Crystallogr. B 38 (1982) 1101.
[160] J.K. Burdett, E. Canadell, J. Am. Chem. Soc. 112 (20) (1990) 7207.
[161] S.C. Sevov, J.D. Corbett, Inorg. Chem. 31 (1992) 1895.
[162] S.C. Sevov, J.D. Corbett, J. Solid State Chem. 103 (1993) 114.
[163] C. Belin, Rev. Chim. Min. 21 (1984) 263.
[164] G. Bruzzone, Acta Crystallogr. B 25 (1969) 1206.
[165] W. Assmus, M. Herrmann, U. Rauchschwalbe, S. Regel, W. Lieke, H. Spille, S. Horn, G. Weber, F. Steglich, G. Cordier, Phys. Rev. Lett. 52 (1984) 469.
[166] R. Hoffmann, C. Zheng, J. Phys. Chem. 89 (1985) 4175.
[167] M. Charbonnel, C. Belin, Nouv. J. Chim. 10 (1984) 595.
[168] C. Belin, J. Solid State Chem. 50 (1983) 225.
[169] M. Charbonnel, C. Belin, J. Solid State Chem. 67 (2) (1987) 210.
[170] D. Flot, L. Vincent, M. Tillard-Charbonnel, C. Belin, Acta Crystallogr. C 54 (1998) 174.
[171] M. Charbonnel, C. Belin, J. Solid State Chem. 64 (1986) 57.
[172] D. Flot, L. Vincent, M. Tillard-Charbonnel, C. Belin, Z. Krist. 212 (1997) 509.
[173] M. Tillard-Charbonnel, N. Chouaibi, C. Belin, J. Lapasset, J. Solid State Chem. 100 (2) (1992) 220.
[174] M. Tillard-Charbonnel, N. Chouaibi, C. Belin, C.R. Acad. Sci. Paris 315 (1992) 661.
[175] A. Chahine, M. Tillard-Charbonnel, C. Belin, Z. Krist. 209 (1994) 542.
[176] M. Tillard-Charbonnel, C. Belin, Mater. Res. Bull. 27 (1992) 1277.
[177] M. Tillard-Charbonnel, A. Chahine, C. Belin, Z. Krist. 208 (1993) 372.
[178] A. Chahine, M. Tillard-Charbonnel, C. Belin, Z. Krist. 210 (1995) 80.
[179] J.K. Burdett, E. Canadell, Inorg. Chem. 30 (1991) 1991.
[180] J.L. Hoard, B. Sullenger, C.H. Kennard, R.E. Hugues, J. Solid State Chem. 1 (1970) 268.
[181] D. von Geist, R. Kloss, H. Follner, Acta Crystallogr. B 26 (1970) 1800.
[182] B. Callmer, Acta Crystallogr. B 33 (1977) 1951.
[183] R.B. King, Inorg. Chem. 28 (1989) 2796.
[184] M. Tillard-Charbonnel, C. Belin, J. Solid State Chem. 90 (2) (1991) 270.

[185] M. Audier, J. Pannetier, M. Leblanc, C. Janot, J.M. Lang, B. Dubost, Physica B 153 (1988) 136.
[186] J.S. Kasper, J. Less Common Met. 47 (1976) 17.
[187] G. Cordier, V. Muller, Z. Krist. 198 (1992) 302.
[188] D. Flot, M. Tillard-Charbonnel, C. Belin, J. Am. Chem. Soc. 118 (1996) 5229.
[189] G. Cordier, V. Muller, Z. Naturforsch. 49b (1994) 721.
[190] G. Cordier, V. Muller, Z. Naturforsch. 50b (1995) 721.
[191] G. Cordier, V. Muller, Z. Naturforsch. 48b (1993) 1035.
[192] S.C. Sevov, J.D. Corbett, Inorg. Chem. 32 (1993) 1612.
[193] W. Carillo-Cabrera, N. Caroca-Canales, K. Peters, H.G. von Schnering, Z. Anorg. Allg. Chem. 619 (1993) 1556.
[194] J.D. Corbett, Struct. Bond. 87 (1997) 157.
[195] M. Tillard-Charbonnel, C. Belin, A. Manteghetti, D. Flot, Inorg. Chem. 35 (1996) 2583.
[196] Z.C. Dong, J.D. Corbett, Inorg. Chem. 35 (1996) 1444.
[197] M. Tillard-Charbonnel, A. Chahine, C. Belin, Z. Krist. 210 (1995) 162.
[198] M. Tillard-Charbonnel, A. Chahine, C. Belin, R. Rousseau, E. Canadell, Chem. Eur. J. 3 (5) (1997) 799.